28415-H006-R0-00

CR 151696

PRELIMINARY DESIGN

OF AN

ORBITER/IUS SEPARATION SEQUENCE

7 March 1978

(NASA-CR-151696) PRELIMINARY DESIGN OF AN ORBITER/IUS SEPARATION SEQUENCE (TRW Defense and Space Systems Group) 61 p HC A04/MF A01 CSCL 22B

N78-22141

Unclas

G3/16 14085

Prepared for

National Aeronautics and Space Administration
Lyndon B. Johnson Space Center

Contract NAS 9-14723

Prepared by

S. W. Wilson
Systems Engineering and Analysis Department

TRW
DEFENSE AND SPACE SYSTEMS GROUP

Houston, Texas

28415-H006-R0-00

PRELIMINARY DESIGN

OF AN

ORBITER/IUS SEPARATION SEQUENCE

7 MARCH 1978

Prepared for
NATIONAL AERONAUTICS AND SPACE ADMINISTRATION
LYNDON B. JOHNSON SPACE CENTER

Contract NAS 9-14723

Prepared by S. W. Wilson

S. W. Wilson, Manager
Shuttle/IUS Proximity
Operations Software Project

Approved by D K Phillips

D. K. Phillips, Manager
Systems Engineering and
Analysis Department

Systems Engineering and Analysis Department

TRW
DEFENSE AND SPACE SYSTEMS GROUP

Houston, Texas

ABSTRACT

An Orbiter/IUS separation sequence to satisfy the assumed requirements of Shuttle Flight 8 was defined for the purpose of gaining an insight into the flight design software requirements of the JSC Mission Planning and Analysis Division. The key to economical and effective flight design for Orbiter/IUS proximity operations appears to be the capability for rapid and accurate generation of graphical displays that will facilitate not only decision-making on the part of the designer, but also lucid documentation of his rationale and of the resulting design features.

The data and the rationale developed in this exercise, which can be regarded at best as only a preliminary step in an iterative process, indicate that (1) an OMS burn is required to attain the necessary departure velocity without subjecting the IUS and its payload to undue plume impingement, and (2) a departure trajectory that places the Orbiter above and behind the IUS at SRM ignition time is preferred over the alternative which would place it below and ahead.

TABLE OF CONTENTS

LIST OF TABLES

LIST OF FIGURES

LIST OF FIGURES (CONT)

LIST OF FIGURES (CONT)

SYMBOLS AND ACRONYMS

ACS	Attitude Control System
CG	Center of gravity (center of mass)
DAP	Digital Autopilot
DoD	Department of Defense
G.E.T.	Ground elapsed time; i.e., time from Shuttle liftoff (hr:min or hr:min:sec)
GTS	Guam Tracking Site
IUS	Inertial Upper Stage
I_{xx}, I_{yy}, I_{zz}	Moments of inertia
I_{yz}, I_{xz}, I_{xy}	Products of inertia
LVLH	Local vertical/local horizontal coordinate system
MPAD	Mission Planning and Analysis Division
OMS	Orbital Maneuvering System
P.E.T.	Phase elapsed time (min:sec)
p, q, r	Angular velocity components about body X, Y, Z axes, respectively
RCS	(Primary) Reaction Control System
RMS	Remote Manipulator System
RTS	Remote tracking site
SBS	Satellite Business System (satellite)
SRM	Solid rocket motor
SSUS	Spinning Solid Upper Stage
STDN	Spaceflight Tracking and Data Network
TDRS	Tracking and Data Relay Satellite
VRCS	Vernier Reaction Control System
X, Y, Z	Cartesian axes or position components
$\dot{X}$, $\dot{Y}$, $\dot{Z}$	Linear velocity components
$\ddot{X}$, $\ddot{Y}$, $\ddot{Z}$	Linear acceleration components

Subscripts

B	Orbiter body axes
O	Orbiter structural body axes
I	IUS body axes

1. INTRODUCTION

This report contains the results of a flight design exercise that was undertaken for the purpose of gaining an insight into detailed software requirements of the JSC Mission Planning and Analysis Division (MPAD), as they pertain to Orbiter/Inertial Upper Stage (IUS) proximity operations. Definition of an Orbiter/IUS separation sequence for Shuttle Flight 8 was taken as a representative flight design task.

The two major items on the Shuttle cargo manifest for Flight 8 are

(1) A Satellite Business System (SBS) satellite mounted on a Spinning Solid Upper Stage (SSUS), and

(2) A Tracking and Data Relay Satellite (TDRS) mounted on a two-stage IUS.

Both satellites are destined for geosynchronous equatorial orbit. The tentative launch date for Flight 8 is 1 July 1980. The SSUS/SBS is to be deployed from the Orbiter about 45 minutes before SSUS solid rocket motor (SRM) ignition, which is scheduled at approximately 4:58 (hr:min) Ground Elapsed Time (G.E.T.). Following the SSUS SRM burn, the IUS/TDRS spacecraft will be checked out and deployed in preparation for the IUS first-stage burn (SRM-1), which is scheduled at approximately 11:00 G.E.T. This report specifically addresses only that phase of the flight that occurs between the release of the IUS/TDRS from the Orbiter's Remote Manipulator System (RMS) and the completion of the IUS SRM-1 burn.

2. ASSUMPTIONS

2.1 GENERAL REQUIREMENTS FOR TDRS PLACEMENT FLIGHTS

Following is a list of the assumed flight design requirements for the Orbiter/IUS separation phase of any TDRS placement flight. These requirements were extracted from a draft of the Flight 8 Conceptual Flight Profile document, which is to be published by MPAD in the near future.

1. The RMS is to be used to deploy the IUS/TDRS from the Orbiter.

2. The earliest permissible time for release of the IUS from the RMS is 45 minutes prior to SRM-1. This is an IUS battery lifetime constraint.

3. The IUS/TDRSS combination is to be protected from direct sunlight during preparations for release. This is a TDRS thermal constraint.

4. A minimum separation distance of 200 feet between the Orbiter and the IUS is required for activiation of the IUS attitude control system (ACS). This is an Orbiter contamination and flight safety constraint.

5. The IUS ACS must be activated no later than 9 minutes after release. This is required so that the IUS can initiate a rotisserie motion to control TDRS temperatures.

6. In the interval between release and activation of the IUS ACS, it is desired to maintain an angle no greater than 30 degrees and no smaller than 10 degrees between the IUS -X axis (℄ of SRM exhaust) and the line of sight to the sun. This is also related to TDRS thermal control.

7. All Orbiter control jets are assumed to be inhibited at the instant of release. Primary Reaction Control System (RCS) jets may not be fired during the first minute after release. This is to allow the RMS to be moved safely away from the IUS/TDRS and rigidized before RCS firing.

8. The Orbital Maneuvering System (OMS) engines may not be fired during the first 10 minutes after release of the IUS/TDRS. This interval is provided to allow the RMS to be stowed and latched down.

9. A minimum separation distance of 10 nautical miles between the Orbiter and the IUS is required before enabling the IUS SRM ignition circuit. This is a flight safety constraint designed to avoid Orbiter damage in the event of SRM detonation.

10. If the necessary communication opportunity exists, the prime mode for enabling the SRM is by direct RF link to the IUS from a Department of Defense (DoD) Remote Tracking Site (RTS). An Orbiter-to-IUS RF link (20 nautical miles maximum range) is available for backup of the RTS command, or for use in case no RTS communication opportunity exists during the appropriate time interval.

11. Plume impingement on the IUS/TDRS from Orbiter thrusters is to be minimized.

12. Damage to the Orbiter from the IUS SRM plume is to be avoided.

2.2 SPECIFIC REQUIREMENTS FOR FLIGHT 8

Following is a list of the assumed flight design requirements and constraints for the Orbiter/IUS separation phase of Shuttle Flight 8. These were also extracted from the previously-cited draft of the Flight 8 Conceptual Flight Profile document.

1. The nominal orbit for deployment of the IUS/TDRS from the Orbiter is circular, with an altitude of 150 nautical miles and an inclination of 28.5 degrees.

2. The nominal TDRS placement longitude, which is to be achieved at SRM-2 burnout, is 55° W.

3. The IUS SRM-1 burn is scheduled to occur at approximately 11:00 G.E.T.

4. Shuttle liftoff is scheduled for 2100 GMT (1600 EST) on 1 July 1980.

5. The DoD and STDN ground stations identified in Table 1 are assumed to be available for communications.

Table 1. Communication Stations

	ID	Station Name	Geodetic Latitude (deg N)	Longitude (deg E)
STDN Network	ACN	Ascension	-7.95	345.67
	AGO	Santiago	-33.15	289.33
	BDA	Bermuda	32.35	295.34
	GBT	Greenbelt	39.00	283.16
	GDS	Goldstone	35.34	243.13
	GWM	Guam	13.31	144.74
	HAW	Hawaii	22.13	200.33
	KWA	Kwajalein (C-Band)	9.40	167.48
	MAD	Madrid	40.46	355.83
	MIL	Merritt Island	28.51	279.31
	ORR	Orroral	-35.63	148.95
	QUI	Quito	-0.62	281.42
DoD Network	GTS	Guam	13.61	144.85
	HTS	Hawaii	21.57	201.74
	IOS	Indian Ocean	-4.67	55.48
	NHS	New Hampshire	42.95	288.37
	TEL-4	Cape Canaveral	28.35	279.31
	TTS	Thule	76.52	291.48
	VTS	Vandenberg	34.82	239.50

3. REQUIREMENTS ANALYSIS

Figure 1 depicts the daylight/darkness timeline, along with ground-station communication opportunities, for the interval of time during which the Orbiter/IUS separation sequence is to be executed during Flight 8. The line of sight to the sun from the Orbiter's position at 10:15 G.E.T. (the nominal time for release of the IUS/TDRS from the RMS) is shown with respect to the local vertical/local horizontal (LVLH) coordinate system in Figure 2. These data correspond to a preliminary Orbiter trajectory that was generated by MPAD on the basis of the Flight 8 requirements that are listed in Section 2.2. Their availability is a necessary prerequisite for the design of a separation sequence that will satisfy the general requirements listed in Section 2.1.

3.1 PARAMETRIC ANALYSIS OF SEPARATION TRAJECTORIES

Before attempting the detailed design of the separation sequence, a parametric analysis of in-plane separation trajectory characteristics was performed. An out-of-plane separation maneuver was considered, but this option was quickly discarded because of the large velocity increment (70 feet per second at the very minimum) that would be necessary to attain the 10 nautical mile separation distance which is required before enabling the SRM ignition circuit.

The basic parameters of interest for an in-plane separation trajectory are

1) the magnitude of the initial velocity increment (DELTA V),

2) the direction of the velocity increment (THRUST ANGLE), and

3) the elapsed time in the separation trajectory (COAST TIME).

The first two parameters are illustrated geometrically in Figure 3. A heads-down OMS burn is depicted there; however, the choice of propulsion unit and Orbiter attitude is irrelevant at this time. The important point is that the thrust angle is measured, positive upward, from the LVLH X axis to the incremental velocity vector.

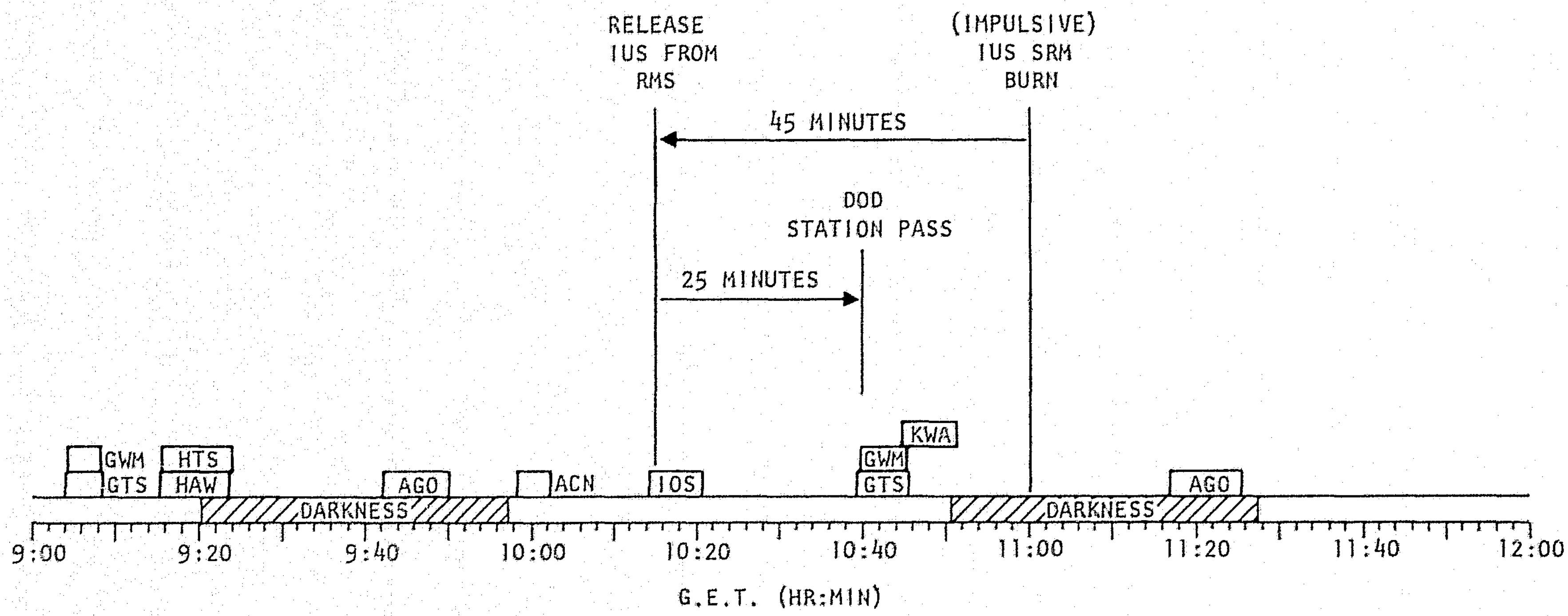

Figure 1. On-Orbit Lighting and Ground Station Passes (Flight 8)

28415-H006-R0-00

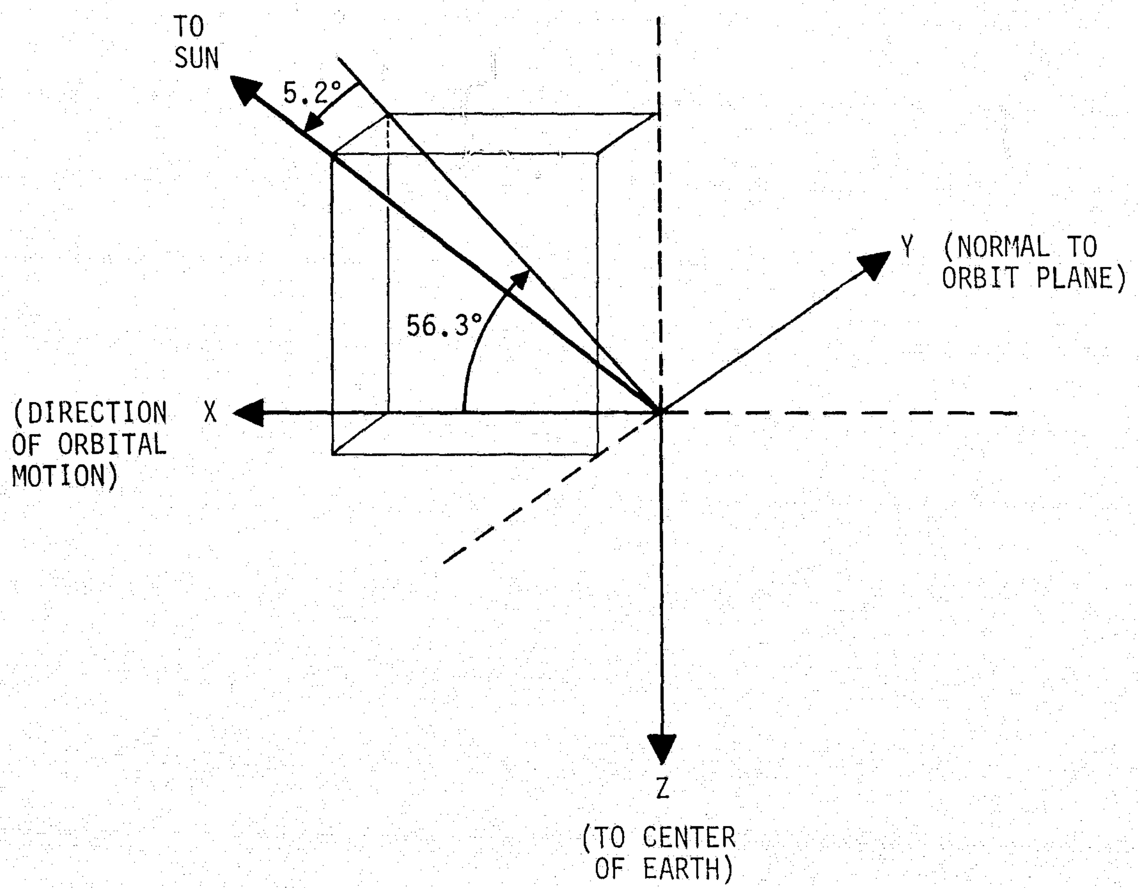

Figure 2. Direction of Sun Relative to LVLH Coordinate System (G.E.T. = 10:15, Orbiter at Origin)

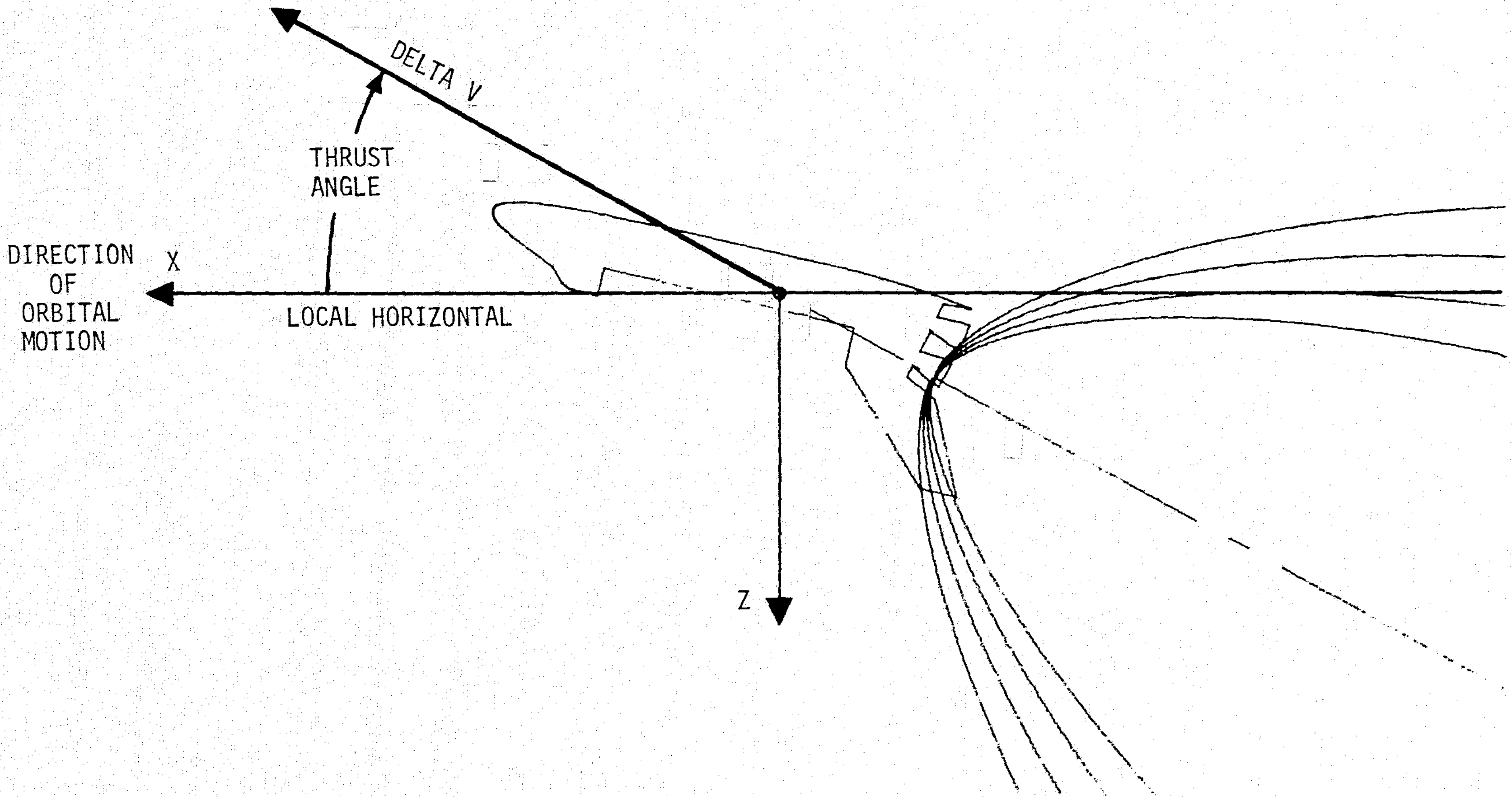

Figure 3. Separation Trajectory Parameters (LVLH Coordinate System)

28415-H006-R0-00

3.1.1 Orbiter ΔV Requirement and Plume Impingement on IUS/TDRS

Figure 4 shows, for an arbitrary velocity increment magnitude of 20 feet per second and a coast time of 24 minutes, the effect of thrust angle on the Orbiter's separation trajectory in a rotating LVLH coordinate system centered on the IUS. The 24-minute coast time is consistent with the use of RCS thrusters for applying the separation velocity increment. It represents the 25-minute interval between release and the beginning of the DoD Guam Tracking Station (GTS) pass (see Figure 1), minus one minute for maneuvering the RMS safely away from the IUS/TDRS and rigidizing it in preparation for the RCS burn.

The most important fact illustrated in Figure 4 is that the thrust angle has a significant effect on the separation distance that can be attained with a fixed coast time and a fixed velocity increment magnitude. The locus of the end points of all trajectories that can be generated by varying the thrust angle (while holding delta V and coast time constant) has the appearance of an ellipse. Figure 5 shows that increasing the velocity increment magnitude while holding the coast time constant has the effect of increasing the size of this "ellipse"* without changing its shape or its orientation relative to the LVLH axes.

The radius of the circle in Figure 5 represents the 10 nautical mile separation distance that must be attained before enabling the SRM ignition circuit. It can be seen that the minimum RCS increment that will produce the required separation in the available time interval is approximately 22 feet per second. There is no way that an RCS translational maneuver of such a magnitude can be executed one minute after releasing the IUS/TDRS from the RMS without subjecting the released spacecraft to severe plume impingement. The reason is illustrated in Figure 6, which depicts the most benign mode (from the plume impingement standpoint) that is available for performing such a maneuver. Assuming all four +X RCS jets to be fired simultaneously†, the thrust acceleration would be approximately 0.6 feet per second, and a

*It has not been determined whether this is a precise characterization of the figure in question.

†This would require a change in the on-orbit digital autopilot (DAP) logic, which currently provides only a two-jet +X RCS translational capability.

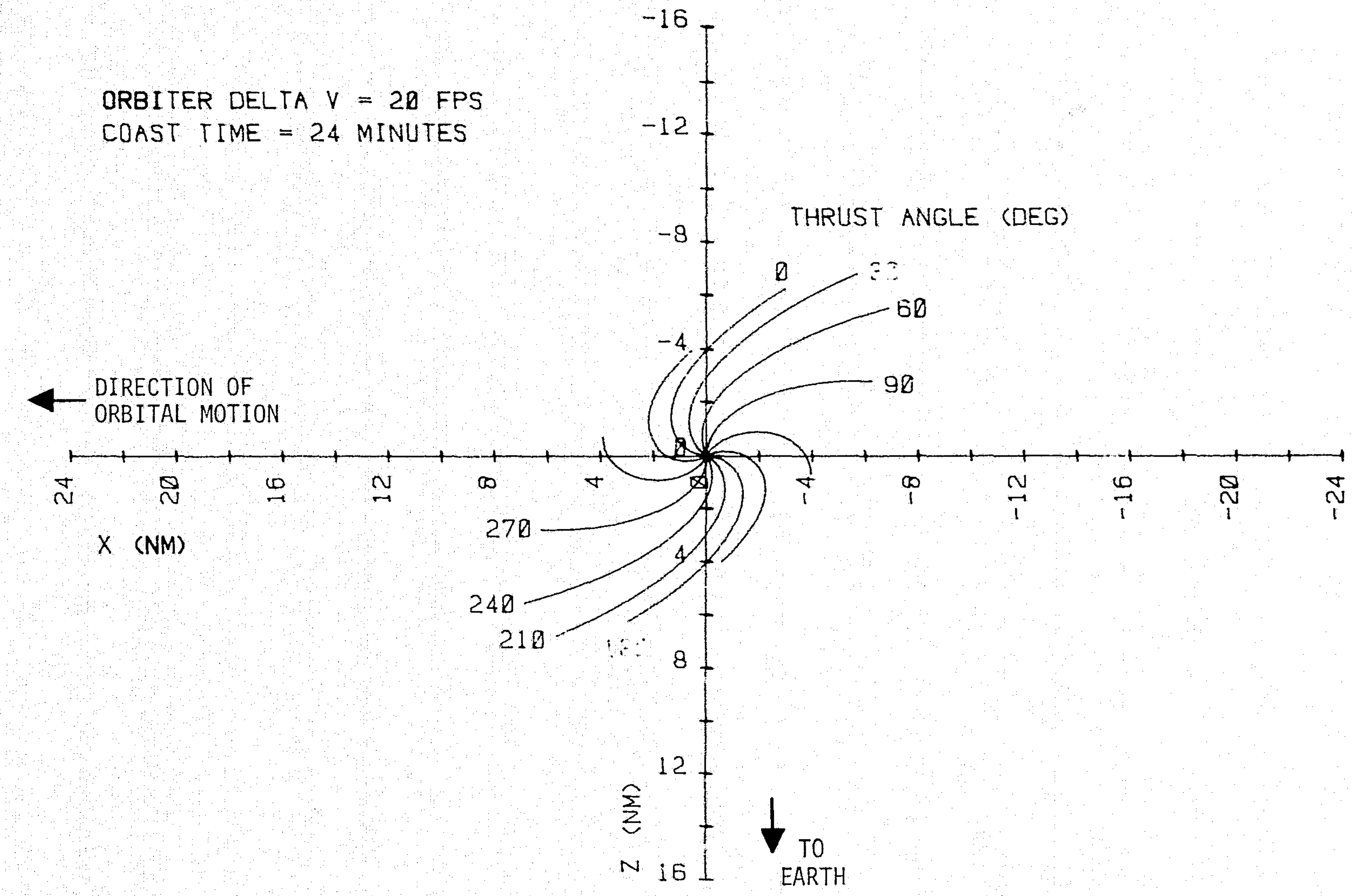

Figure 4. Typical Separation Trajectories (Rotating Coordinate System, IUS at Origin)

28415-H006-R0-00

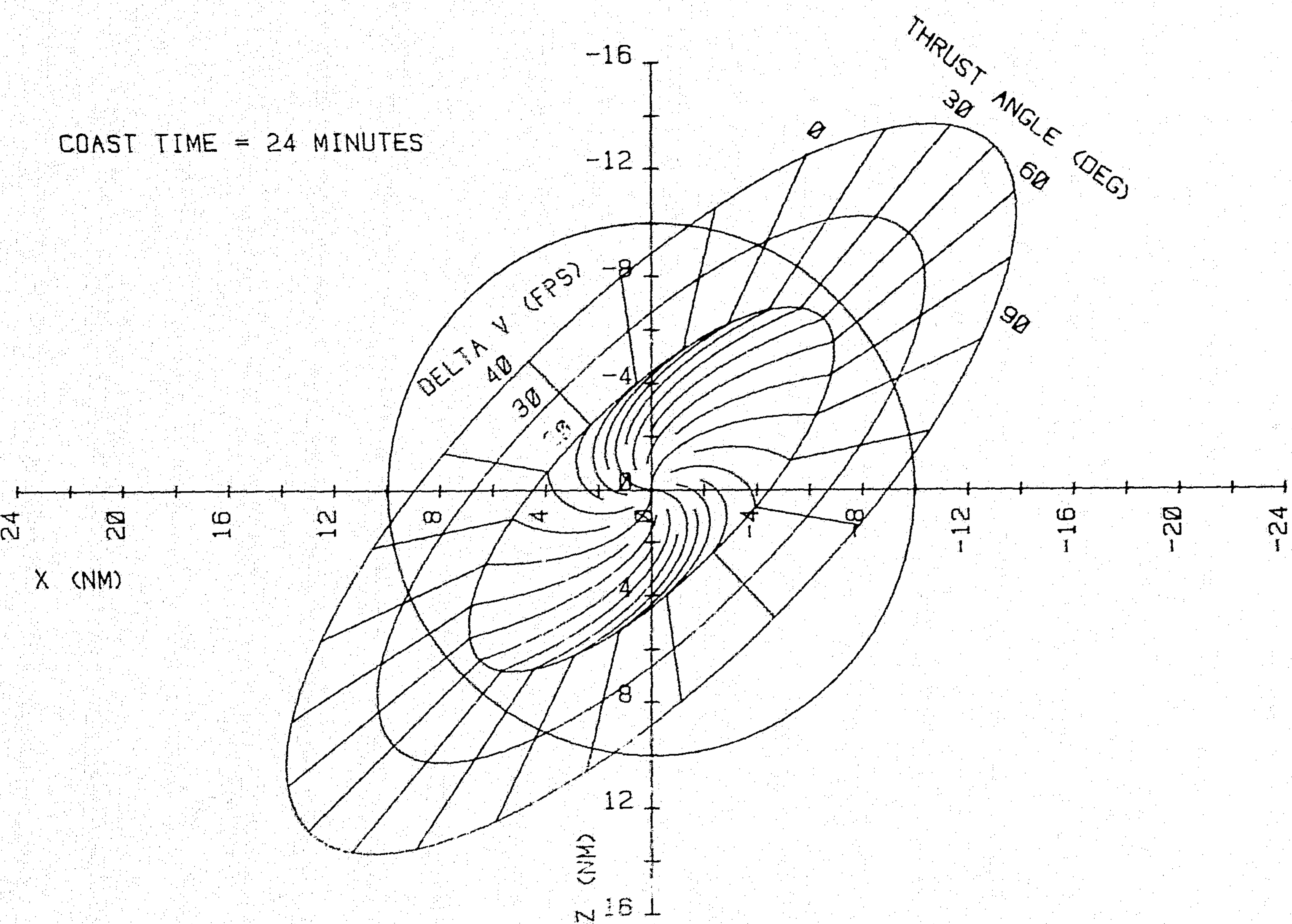

Figure 5. Effect of Delta V Magnitude (RCS Main Separation Burn)

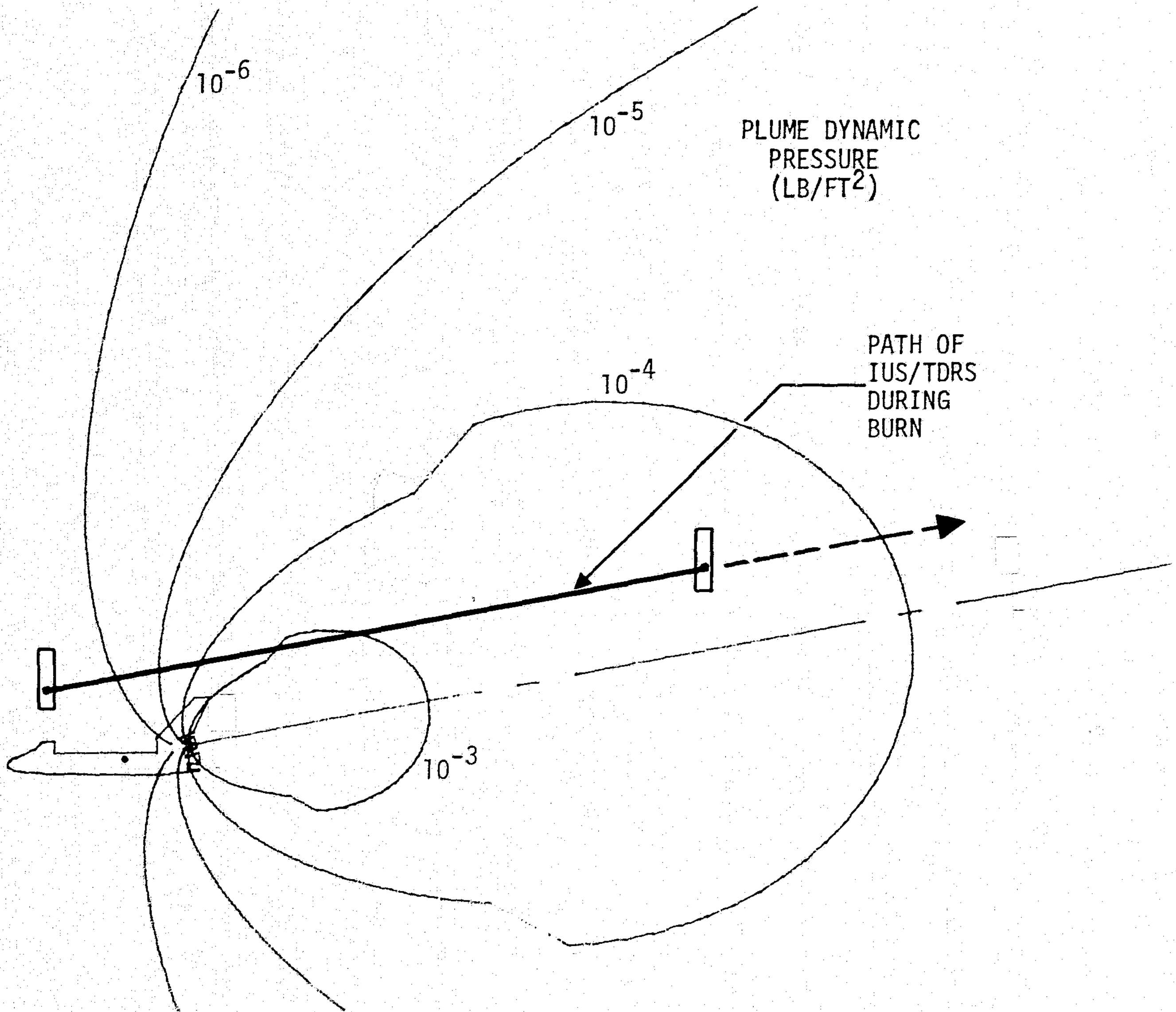

Figure 6. RCS Sep Maneuver Executed One Minute After Release

28415-H006-RO-00

burn time of approximately 37 seconds would be necessary to realize a velocity increment of 22 feet per second. As shown in Figure 6, the IUS/TDRS would traverse a flight path of roughly 400 feet relative to the Orbiter during the burn, and would be deeply immersed in the RCS plume.

The severity of the plume impingement effect might be reduced if it were permissible to fire the OMS engines one minute after release of the IUS/TDRS from the RMS*; however, it would still be almost certainly unacceptable. As illustrated in Figure 7, the shorter flight path traversed by the released spacecraft during the burn (approximately 120 feet) would still be long enough to produce significant impingement effects.

Figures 6 and 7 indicate a need for the Orbiter to back away from the released spacecraft (by means of a -X RCS impulse) before execution of the main separation burn. The purpose of the initial impulse is to shift the position of the IUS/TDRS forward relative to the Orbiter body axes, and thereby to avoid immersing it in the thruster plume during the main separation maneuver. The initial impulse must itself be small (probably no greater than 3 feet per second) to avoid unacceptable impingement on the IUS/TDRS by the -X RCS plume.

Since the initial impulse must be small, a significant time interval will be required to attain the separation distance needed to avoid excessive impingement during the main burn. Time is also needed to execute an Orbiter rotational maneuver, since the optimum attitude for the main burn is not consistent with the release attitude which is necessary to meet the TDRS thermal control requirements. The situation is complicated by the fact that every second of delay in executing the main separation burn must be subtracted from the post-burn coast time that is available for attaining the 10 nautical mile separation distance which is required for enabling the SRM during the GTS pass. This in turn increases the magnitude of the required main-separation velocity increment and therefore the length of the Orbiter-relative flight path traversed by the IUS/TDRS during the burn. Thus: the longer the delay, the greater the distance that must be put between the Orbiter and the released spacecraft during the delay.

*The maximum dynamic pressure experienced by the IUS/TDRS would be about the same, or possibly a little higher, but the exposure time would be considerably shorter.

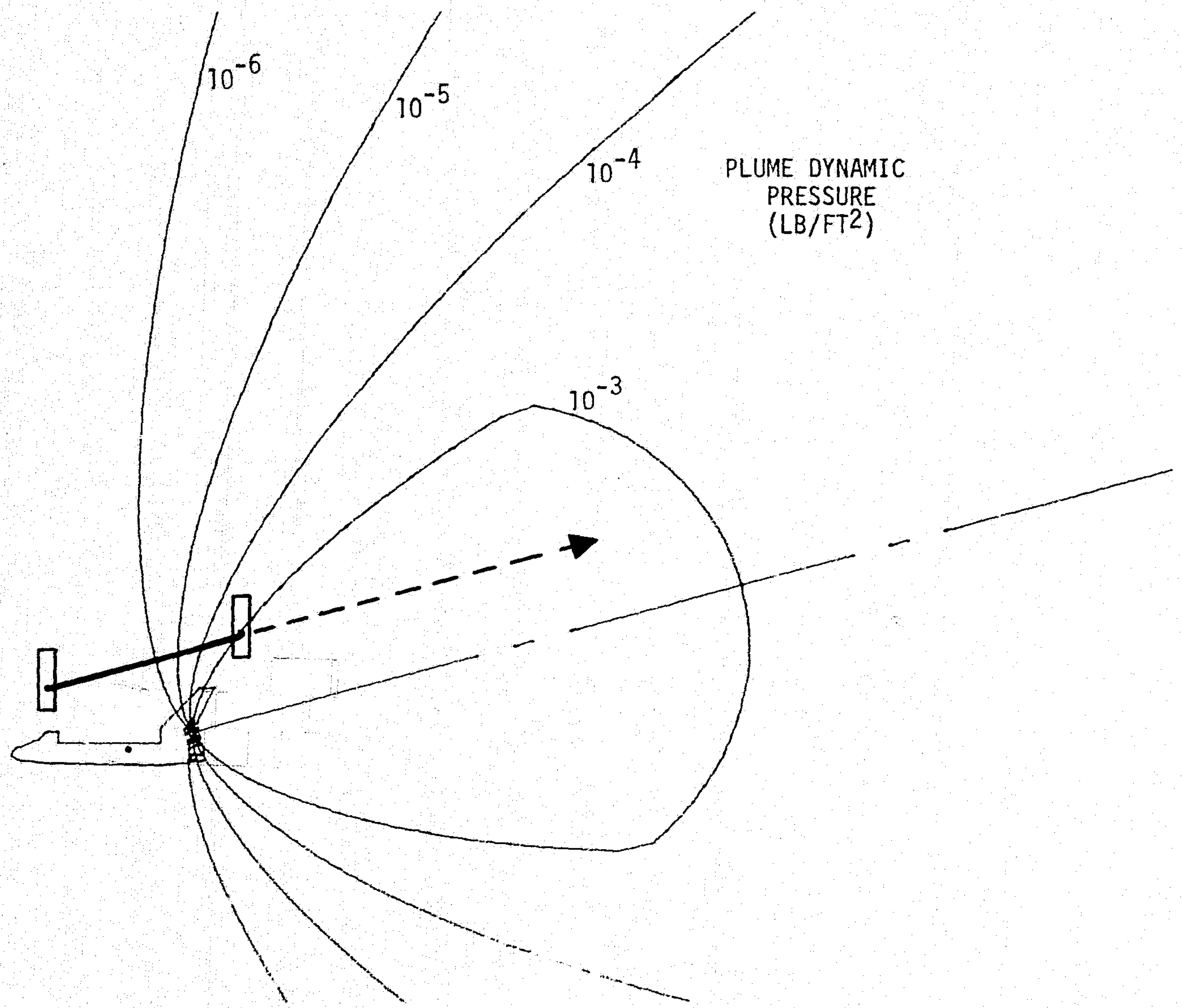

Figure 7. OMS Sep Maneuver Executed One Minute After Release

28415-H006-R0-00

Although a detailed analysis of tradeoffs between the durations of the coast intervals before and after the main separation burn might lead to the design of an acceptable separation sequence which uses only RCS thrusters, rough calculations indicate that simultaneous firing of 4 +X jets would be necessary. Since this would require a modification of the on-orbit DAP logic, it was decided to base the design of the separation sequence on the use of the OMS engines for the main burn*.

Figure 8 shows, for a coast time of 15 minutes, the effect of velocity increment magnitude on the locus of IUS-relative positions accessible to the Orbiter. The 15-minute coast time is compatible with an OMS burn. It represents the 25-minute interval between IUS release and the beginning of the GTS pass, minus a 10 minute allowance for stowing and latching down the RMS. By comparing Figures 5 and 8, it can be seen that decreasing the coast time rotates the "ellipse" (the quotation marks are used because it still has not been determined that the figure in question is truly an ellipse) and reduces its eccentricity. It can also be seen that there is a significant difference in the optimum thrust angle.

Figure 8 indicates that an OMS velocity increment of slightly under 50 feet per second is needed to satisfy the distance requirement for enabling the SRM. A nominal value of 48 feet per second was chosen for detailed trajectory design purposes. Figure 9 shows, at five minute intervals measured from the time of the main separation burn, the locus of positions which are accessible to the Orbiter with such a velocity increment magnitude. The maximum coast time for which data are shown in Figure 9 (35 minutes) represents the approximate interval between the main separation burn and SRM-1 ignition.

*Using the -Z jets to execute the main burn would yield probably enough acceleration to produce acceptably small impingement effects without modifying the DAP logic, but this option was discarded because of poor propellant economy.

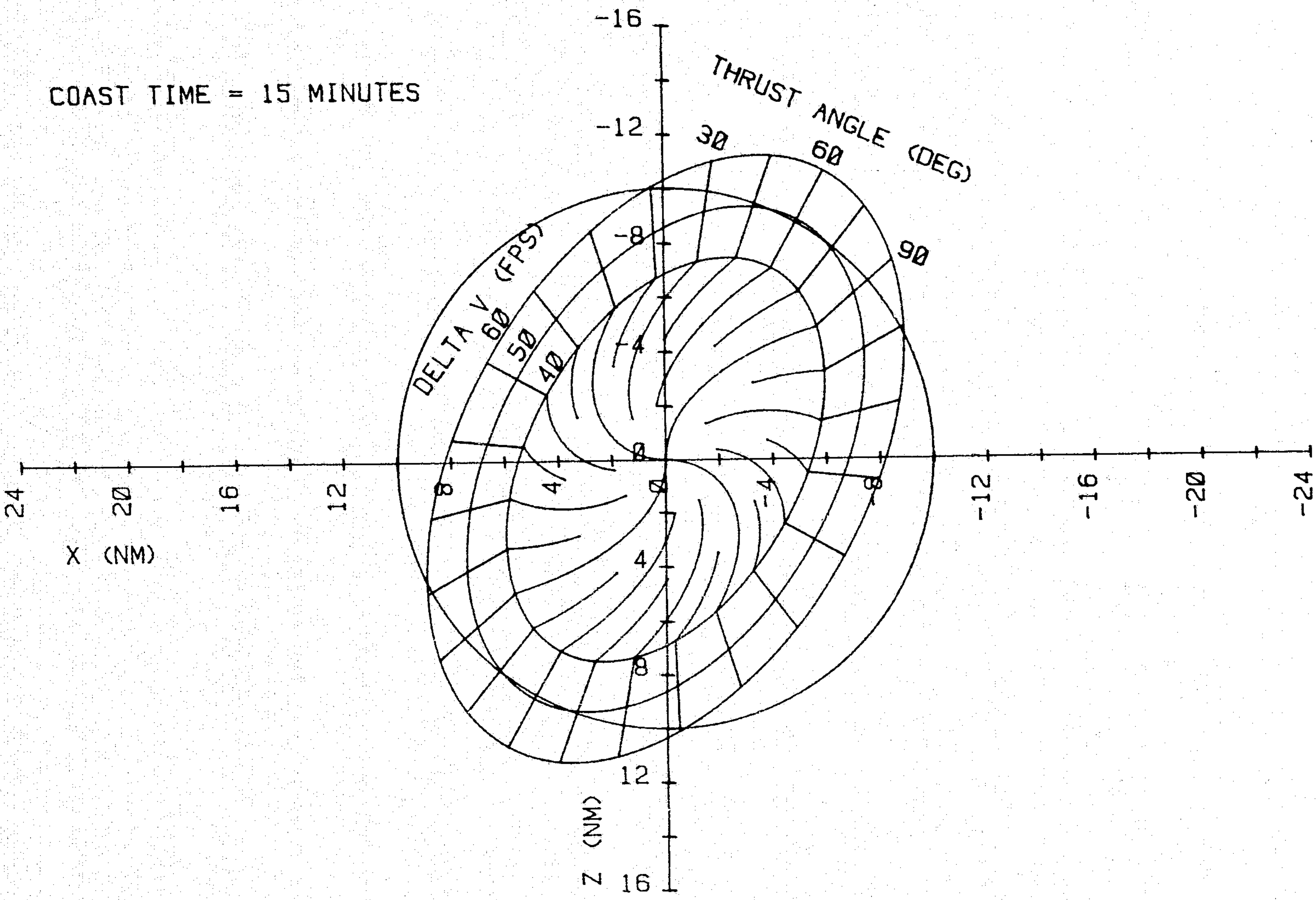

Figure 8. Effect of Delta V Magnitude (OMS Main Separation Burn)

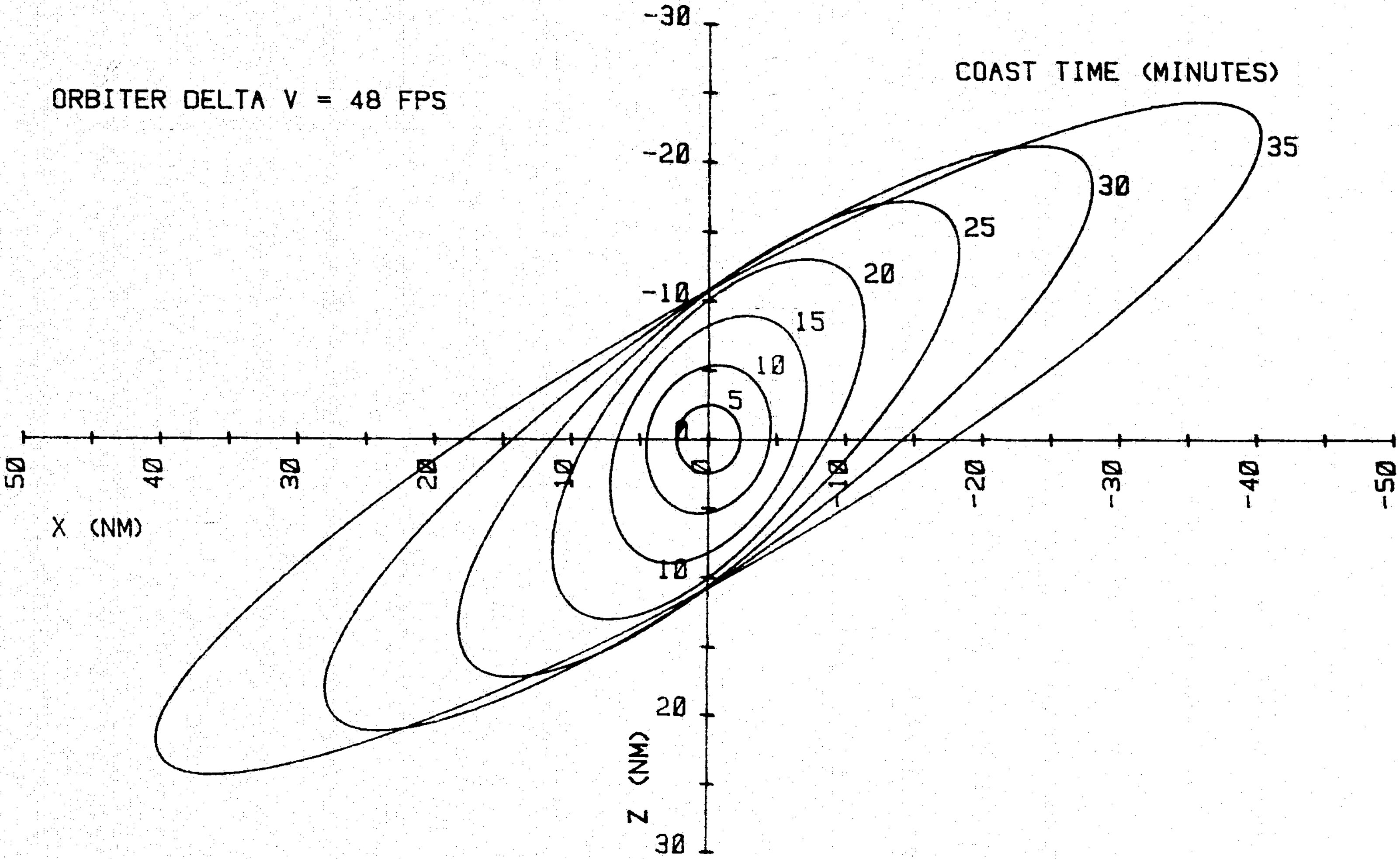

Figure 9. In-Plane Positions Accessible to Orbiter

3.1.2 IUS SRM Plume Impingement on Orbiter

Having determined the trajectory characteristics needed to avoid excessive Orbiter plume impingement on the IUS/TDRS and to provide the required separation distance at SRM enable time, the next question to be addressed is whether these characteristics are compatible with the avoidance of Orbiter damage from the SRM plume.

The first type of potential damage to be considered is that which might be caused by excessive plume dynamic pressure acting on the Orbiter's cargo bay doors, which are assumed to remain open during the SRM-1 burn. In the absence of either a definitive dynamic pressure model or a load limit on the open doors, rough calculations were made which indicated that an Orbiter-IUS separation distance of 7 nautical miles would suffice to attenuate the centerline dynamic pressure of the SRM-1 plume to a value of 3.5×10^{-5} pounds per square foot. The latter value corresponds to the dynamic pressure of the 1962 Standard Atmosphere acting on the Orbiter at the IUS deployment altitude. It is concluded that the effect of the SRM-1 plume dynamic pressure is negligible at any distance greater than 7 miles, and probably of no concern at one tenth of that distance.

The presence of solid particles in the SRM plume makes it necessary to consider other types of damage. Approximately 34% of the mass flux in the SRM-1 exhaust plume consists of aluminum oxide particles. According to References 1 and 2, the diameters of these particles are distributed in the range of 0.0178 to 10 microns, their speeds relative to the IUS in the range of 9850 to 12200 feet per second, and their ejection angles relative to the plume centerline in the range of 0 to 54 degrees. Approximately 0.25% of the mass flux will consist of carbon eroded from the SRM nozzle. If this carbon remains in particulate form,* diameters could range between 17.8 and 1000 microns, IUS-relative speeds between 1600 and 8720 feet per second, and ejection angles between 15 and 30 degrees.

*The size distribution or even the existence of carbon particles is not yet firmly established. However, prudence demands that their effects be considered at least until it can be shown that either (a) they do not exist, or (b) their existence does not represent a hazard to the Orbiter.

Depending on its mass, impact speed, and incidence angle, any of the aforementioned particles can create a pit in one of the Orbiter's windows or thermal protection tiles. In the terminology of Reference 2, damage caused by the less energetic particles is classified as erosion, and that caused by the more energetic particles is classified as breakage.

In the case of a thermal tile, a break represents a penetration of its silicon surface. A window break represents a pit of such a depth (46 microns or more) that thermal stress will cause crack propagation during the subsequent atmospheric entry phase of the Orbiter's flight. According to Reference 1, the energies required to penetrate the surface of a low-temperature tile and a high-termperature tile are, respectively, 84 and 675 times greater than that required to produce a 46 micron pit in a window. Calculations indicate that almost none of the aluminum oxide particles have sufficient energy to break a window, much less a tile. Breakage is therefore a phenomenon that is associated almost exclusively with the postulated carbon particles in the SRM exhaust. The damage-avoidance criterion proposed in Reference 2 for both tiles and windows is that the number of breaks resulting from a single SRM-1 firing should not exceed that which could be expected from meteoroids during a 7 day period of orbital flight. This amounts to some value between 0.06 and 0.28 breaks per square foot of window surface, and somewhere between 0.001 and 0.01 breaks per square foot of thermal tile surface.

Erosion damage is measured in terms of the percentage of surface area affected by the shallow pits which are produced by the less energetic particles. Since their number is so very much greater that that of the carbon particles, the aluminum oxide particles are the primary agents in this type of damage. Erosion changes the thermal properties of tile surfaces, and degrades visibility through the windows. Reference 2 proposes that tile erosion be limited to 10%. This is understood to be a cumulative limit for the lifetime of the tile; therefore, a limit on the order of 0.5% or less per SRM firing would seem appropriate. Reference 2 states that 1% erosion of window surfaces is not expected to be noticed by Orbiter flight crews, that they will begin to complain of reduced visibility at the 2% level, and that it will be impossible under many conditions to see through the windows when 10% of the surface is eroded. It is concluded that the window erosion limit should be on the order of 0.05% or less per SRM firing.

Figure 10 shows, as a function of the Orbiter's position relative to the IUS at the instant of ignition for a representative SRM-1 burn, the percentage of surface erosion (integrated over the duration of the burn) to be expected on window and tile surfaces that are exposed to the SRM plume. Figures 11, 12, and 13, respectively, show the amount of breakage to be expected on exposed window, low-temperature tile, and high-temperature tile surfaces. In all cases the particle incidence angle is assumed to be zero (i.e., the surface orientation is assumed to be normal to the flight path of the impinging particle); however, the relevant impact phenomena are insensitive to incidence angle variations up to a few tens of degrees.

The data shown in Figures 10 through 13 were obtained from References 3 and 4. The IUS flight path during the burn was integrated numerically. The effects of thrust and mass flow rate variations during the burn were modeled. The IUS pitch and yaw angles relative to the LVLH axes were -4.2 and 0 degrees, respectively, at the time of ignition*, and its inertial attitude was held constant throughout the burn. The resulting impulsive-equivalent (mean) LVLH pitch angle was near zero. The orbit of the Shuttle and the pre-ignition orbit of the IUS were assumed to be circular at the appropriate altitudes. Particle trajectories were assumed to be linear; i.e., the effects of gravity and atmospheric drag were not modeled.†

In most cases (Figure 11 is an exception), impingement data were generated only for Orbiter positions in the lower left and upper right quadrants of the LVLH X-Z coordinate frame. The dashed contour lines in the other two quadrants of Figures 10, 12, and 13 were obtained by reflecting the data from

*This is approximately the pitch angle currently planned for SRM-1 ignition in Flight 8. The magnitude of the actual yaw angle is expected to be in the neighborhood of 8 degrees.

†Rough calculations indicate that gravitational acceleration of the larger (low-speed) particles might noticeably alter the shapes of the breakage countours shown in Figure 11 at ranges on the order of tens of miles.

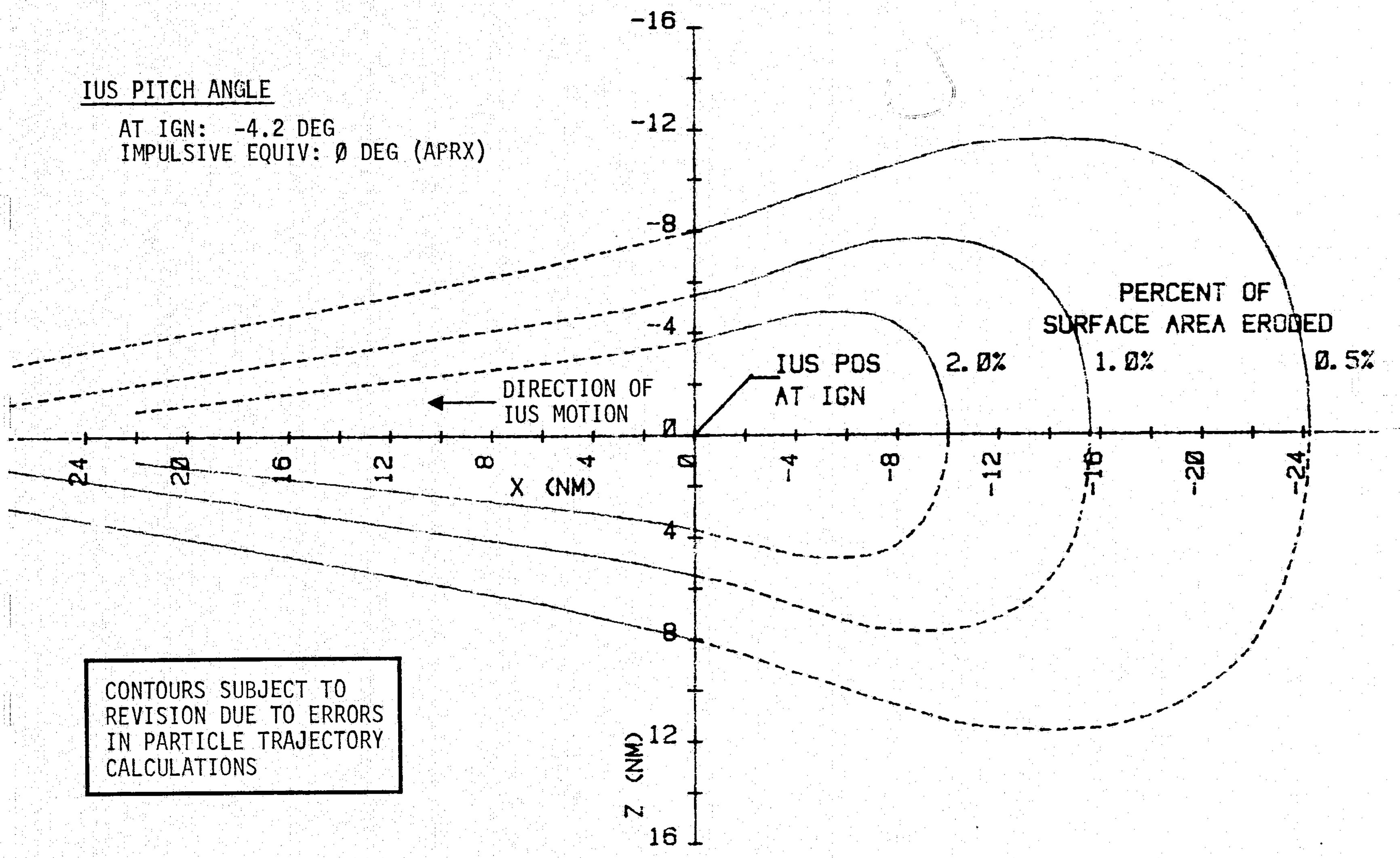

Figure 10. Orbiter Surface Erosion Due to Typical IUS SRM-1 Burn

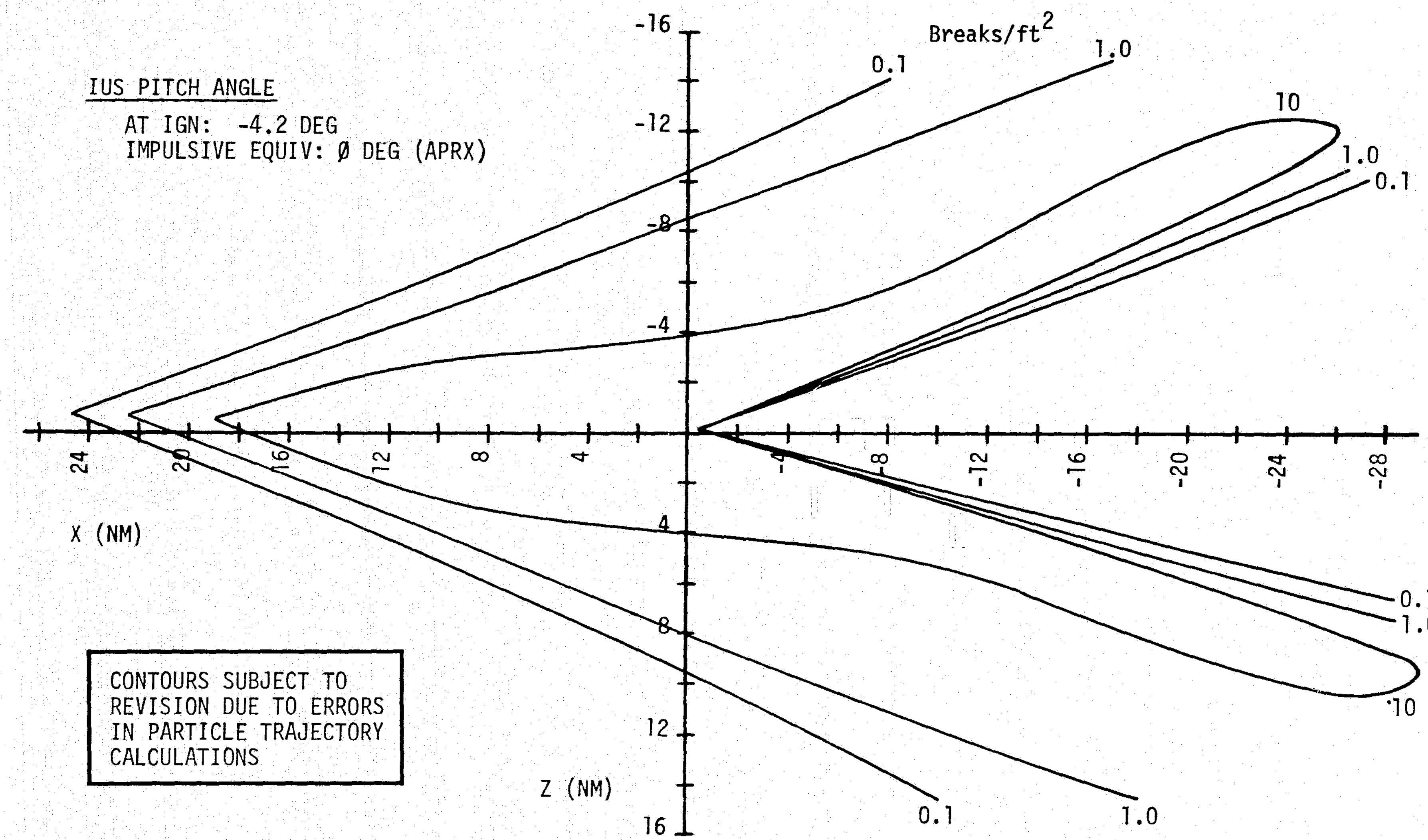

Figure 11. Window Breakage Due to Typical IUS SRM-1 Burn

28415-H006-R0-00

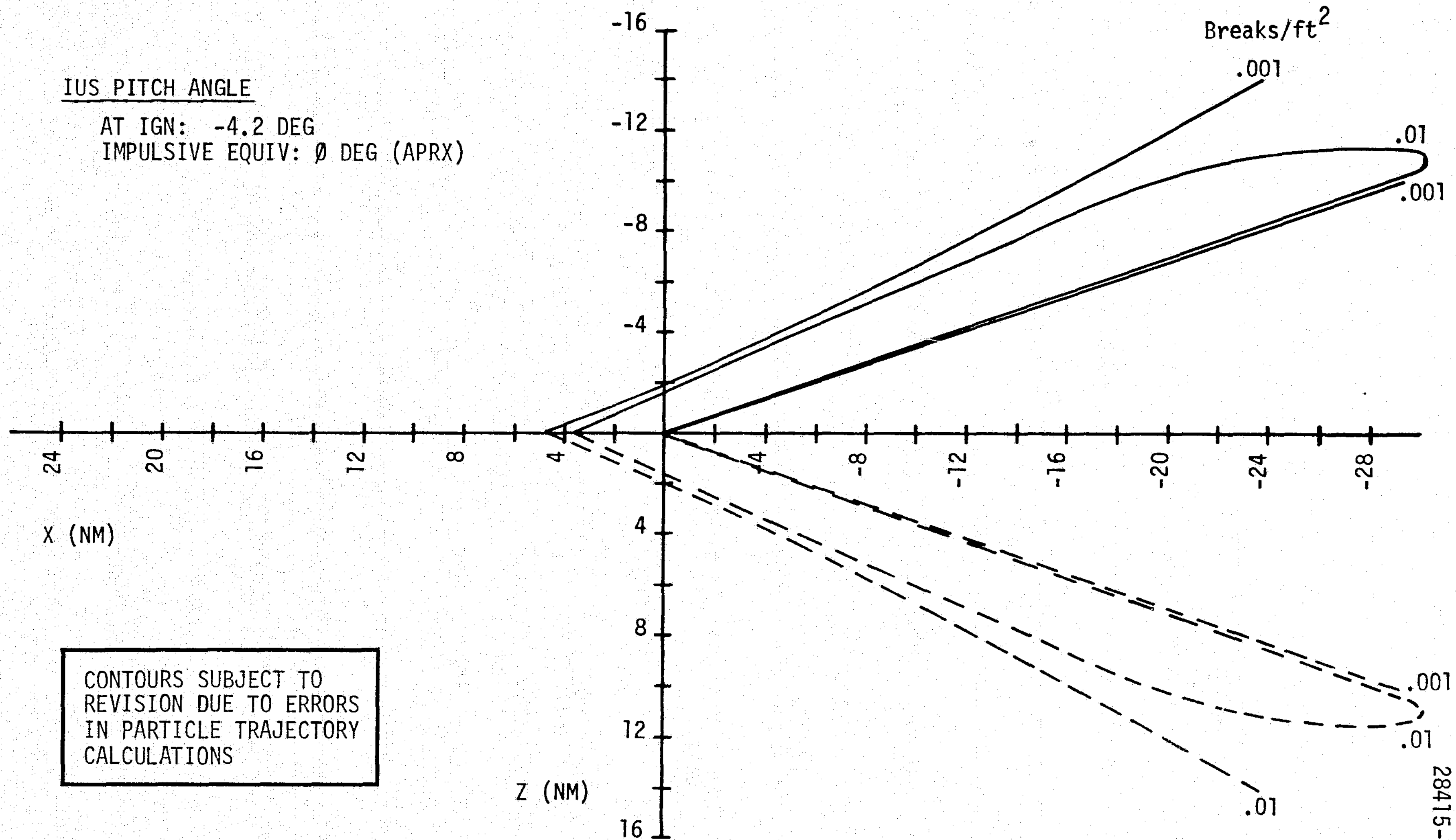

Figure 12. Low-Temperature Tile Breakage Due to Typical IUS SRM-1 Burn

28415-H006-R0-00

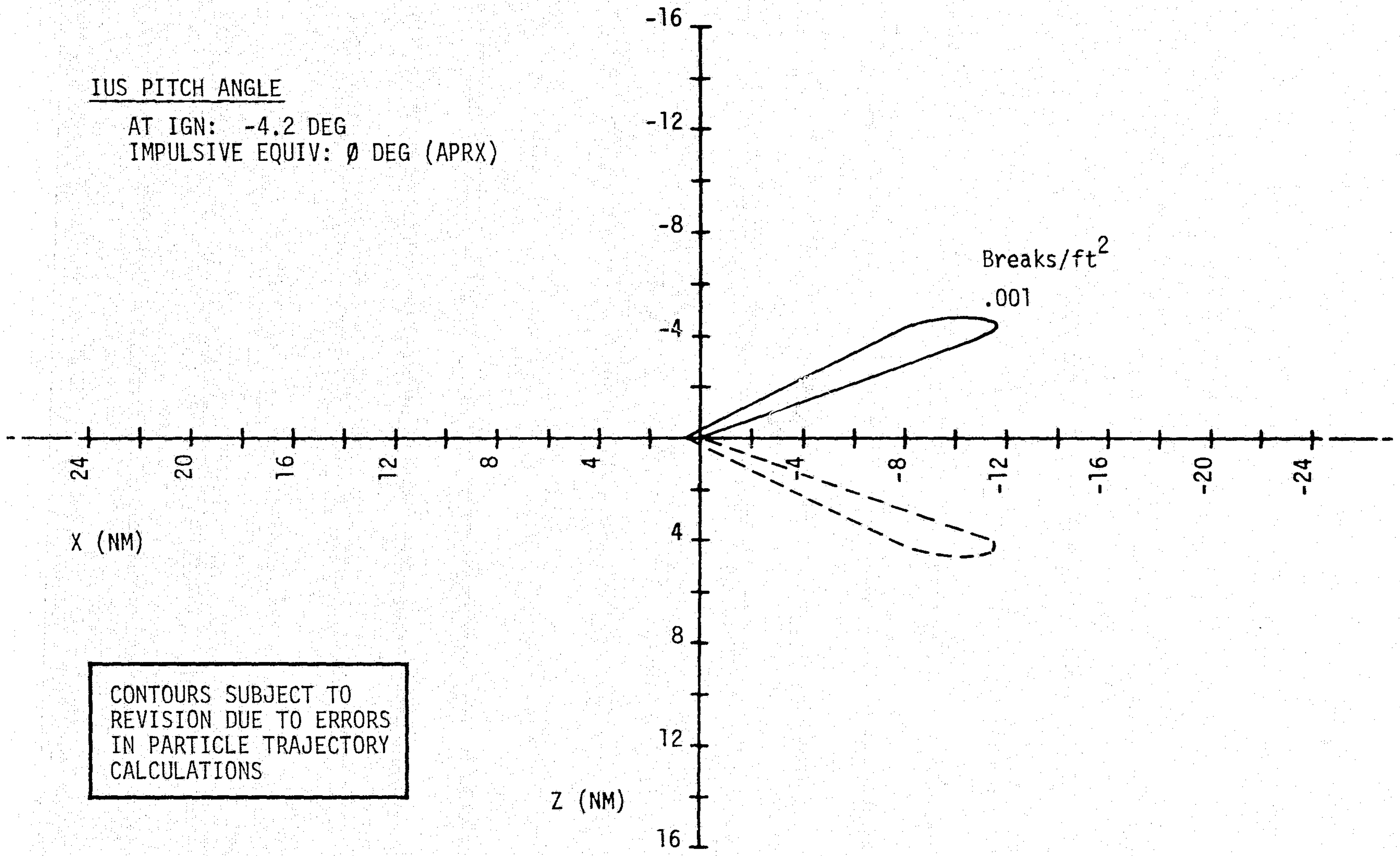

Figure 13. High-Temperature Tile Breakage Due to Typical IUS SRM-1 Burn

the vertically-opposed quadrant about the X axis. Undoubtedly this is an oversimplification of the true figure, but it is believed to be valid at least in an approximate sense. By the same token, three-dimensional approximations of the erosion and breakage environments can be visualized by mentally rotating the contour curves in Figures 10-13 about the LVLH X axis to generate axially symmetric surfaces.

After the data in References 3 and 4 were generated, errors were detected in the equations that were used to transform IUS-relative particle velocities and fluxes to Orbiter-relative values. The magnitude of the error increases with (1) the ratio of the Orbiter-relative IUS speed to the IUS-relative particle speed, and (2) the angle subtended by the plume centerline and the particle's IUS-relative velocity vector. The contour shapes shown in Figures 10-13 are believed to be valid representations of the erosion and breakage environments at least in a qualitative sense; however, the contours need to be reconstructed accurately after completion of the computer program corrections that are now in progress. The contours should be least affected at the far right of Figures 10-13, where the major portion of the erosion and breakage accumulates early in the SRM burn. The magnitude of changes resulting from the corrections should increase from right to left, more so in the case of the breakage (which is caused by the larger low-speed particles) than in the case of erosion (which is caused mainly by the smaller high-speed particles).

3.2 SELECTION OF DEPARTURE QUADRANT

In Figure 14, the SRM-1 erosion contours from Figure 10 have been superimposed on the Orbiter accessibility contours that were previously shown in Figure 9. Minimization of the OMS velocity increment* needed to attain the required 10-mile separation distance at SRM enable time dictates a thrust angle either in the range of 45-75 degrees, or else in the range of 225-255

*Plume impingement on the IUS/TDRS is perhaps more critical in this respect than propellant consumption.

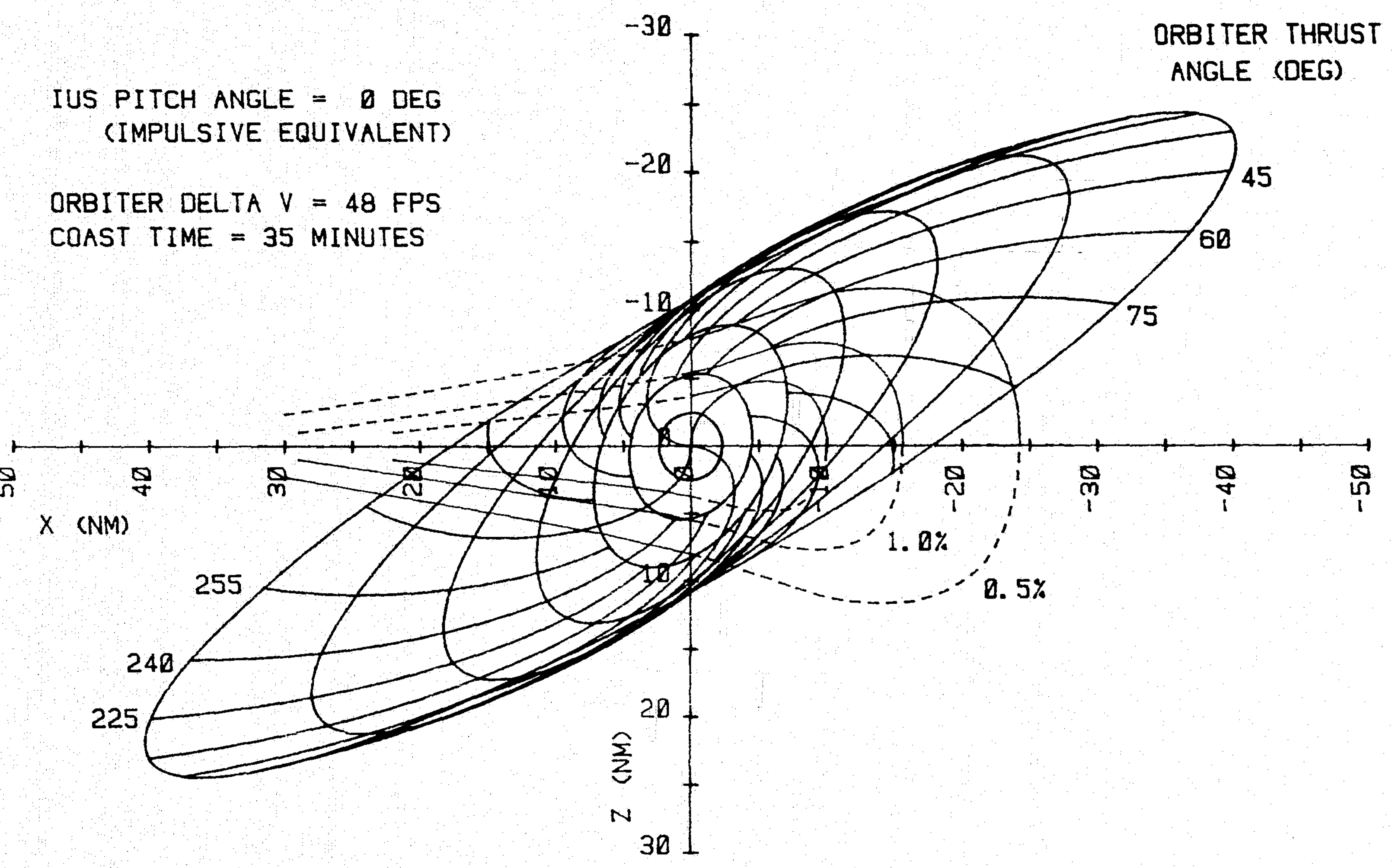

Figure 14. Orbiter Accessibility and Surface Erosion Contours (Baseline IUS SRM-1 Burn)

28415-H006-R0-00

degrees. The first choice will cause the Orbiter to depart from the IUS/TDRS into the upper right quadrant of Figure 14 (above and behind the IUS); the second will cause it to depart into the lower left quadrant (below and ahead).

In favor of the lower left quadrant we have the facts that

(1) this choice will reduce the orbital energy of the Shuttle, thereby tending to decrease the magnitude of its subsequent deorbit velocity increment*, and

(2) Figure 14 indicates that the erosion environment would be more benign. The same is true of the breakage environments, as represented in Figures 11-13.

The magnitude of the first advantage has not been determined. In any event, the weight it should be accorded will depend on an analysis of the OMS propellant budget for the overall flight, which is beyond the scope of present considerations.

In connection with the second argument of the preceding paragraph, it must of course be taken into account that correction of the computer program errors discussed in Section 3.1.2 is expected to change the erosion and breakage contours to a greater extent (and more adversely) there than in the upper right quadrant. However, the general shape of the erosion contours is believed to be sufficiently representative of the true environment to support the following arguments against a departure into the lower left quadrant, which are deemed to be more persuasive than those previously cited.

First of all, the lower left quadrant is considered to be more hazardous in the event of a malfunctioning IUS guidance and control system. This is predicated on the assumption that small deviations from the planned flight path are more probable than large ones in such a case. In this regard it should

*Assuming there are not postdeployment flight objectives that would require transferring the Shuttle to a higher orbit.

be borne in mind that an actual collision is by no means necessary to inflict unacceptable or perhaps even catastrophic damage on the Orbiter. During the nominal SRM-1 burn the IUS traverses a distance on the order of 100 miles roughly along the X axis of Figure 14. If it should pitch downward as in Figure 15* so that it misses the Orbiter by only (say for instance) half a mile, then its plume might very well cause severe erosion and window breakage. It is obvious from inspection of these two figures that the erosion environment in the upper right quadrant, on the other hand, is insensitive to IUS pitch variations of considerable magnitude.

At first it might seem easy to realize an adequate degree of insurance against the effects of a near miss in the lower left quadrant by orienting the Orbiter so that only its less vulnerable belly, which is protected by high temperature tiles, would be exposed to particle impingement. Such a strategem will work in the upper right quadrant†, where the relative flight paths of all the particles that strike the Orbiter are rather closely aligned with each other. However, as indicated in Figure 16, in the lower left quadrant the Orbiter can be struck almost simultaneously by particles approaching from directions that differ by nearly 180 degrees if its position lies near the IUS flight path.

The second argument against a departure into the lower left quadrant, although based on geometrical considerations of a similar nature, has more to do with IUS operational flexibility and flight phase standardization than with the possibility of a guidance and control system malfunction. Any significant degree of standardization in the case of the Orbiter/IUS separation phase probably will require at least that the Orbiter depart consistently, in all IUS deployment flights, into one or the other of the quadrants in question.

*In that figure is is assumed that a reasonable representation of the erosion environment is obtained by rotating the appropriate contours about the LVLH origin, by the amount of the IUS pitch angle difference.

†In fact, it appears to be absolutely essential there; not as insurance against an IUS malfunction, but to protect windows against the severe breakage environment that will attend a nominal SRM-1 firing (see Figure 11).

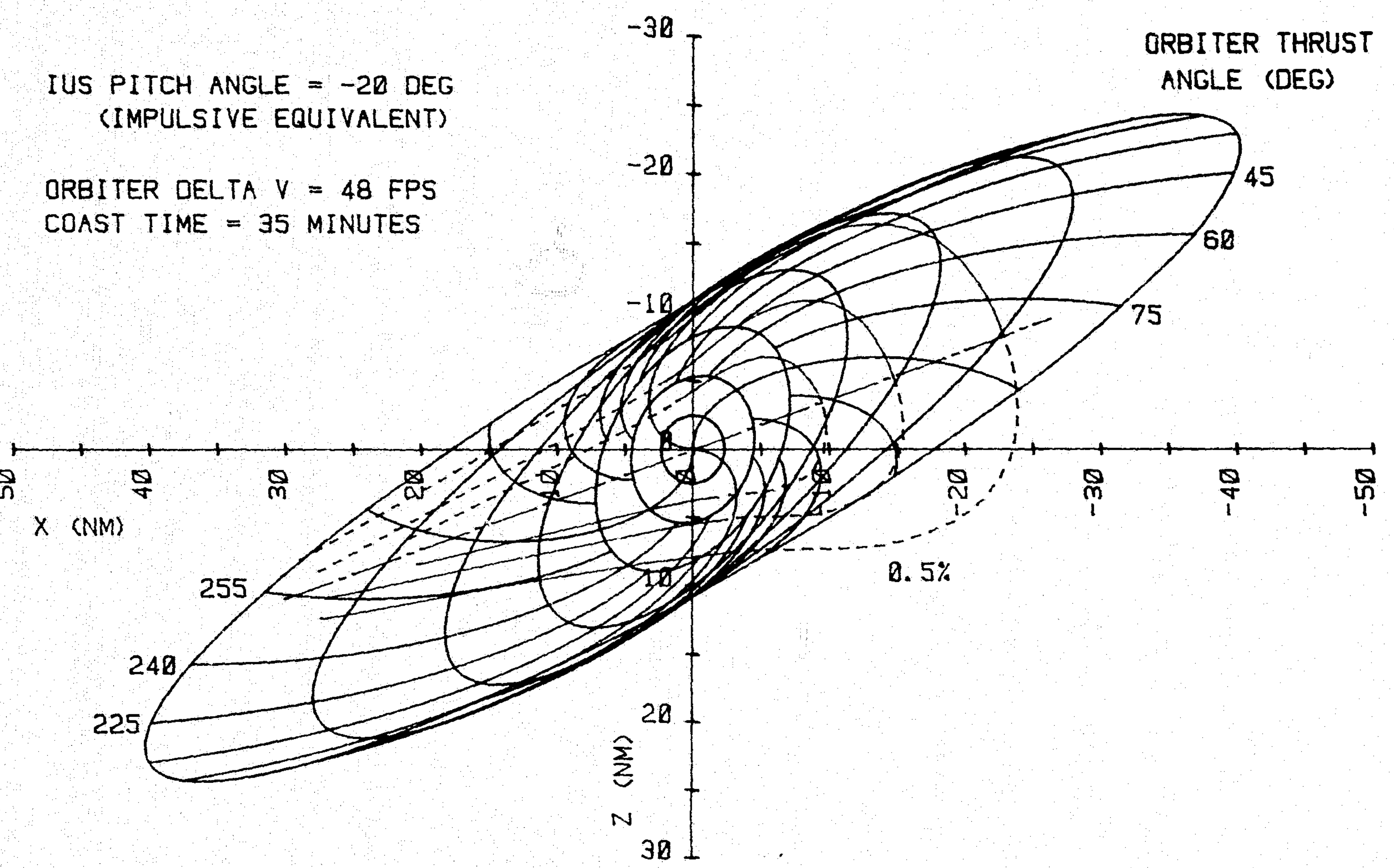

Figure 15. Orbiter Accessibility and Surface Erosion Contours (IUS SRM-1 Burn with Negative Pitch Angle)

28415-H006-R0-00

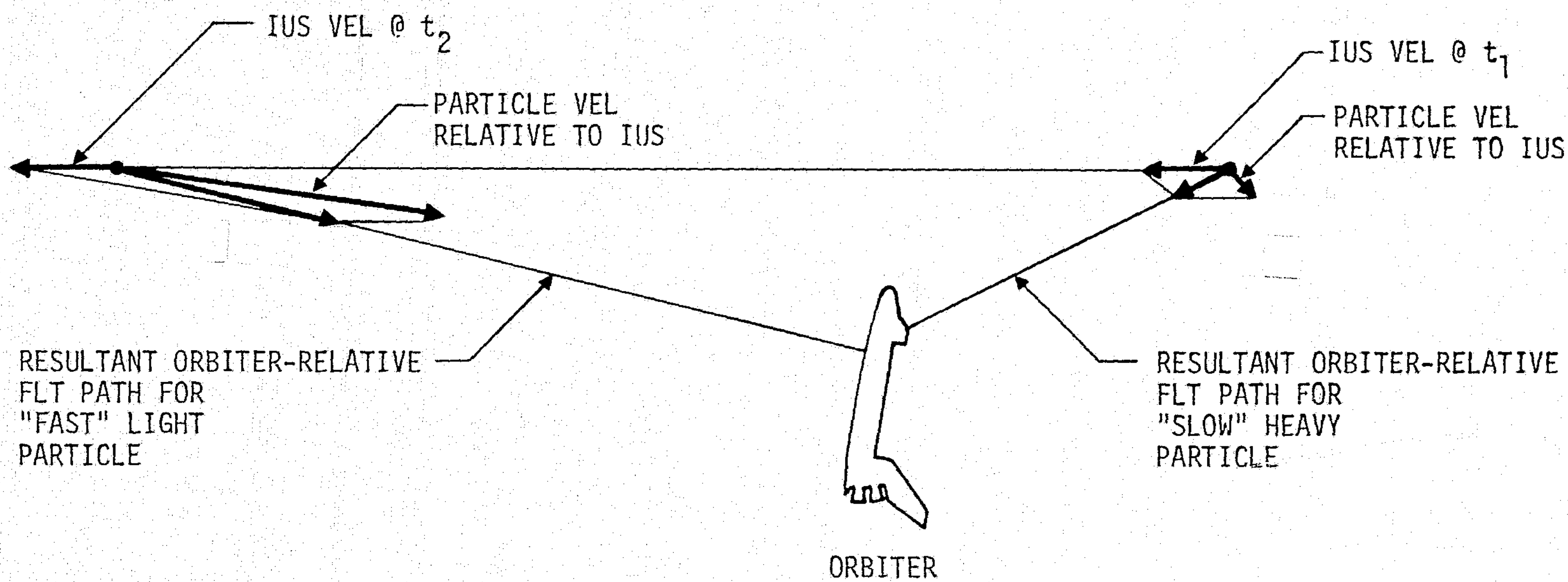

Figure 16. Particle Impingement Trajectories for an Orbiter Position in the Lower Left Quadrant

Selection of the lower left quadrant could result in a 50% reduction of flight planning flexibility, measured in terms of the number of acceptable IUS trajectories from which a nominal flight path can be chosen.

Depending on the weight and destination of its payload for a given flight, the IUS generally will be required to waste more or less of its fixed SRM-1 total impulse by thrusting in a non-optimum direction.* Generally there are 16 discrete solutions to the SRM burn targeting problem. The magnitude of the mean SRM-1 pitch angle tends to be nearly identical in all 16 solutions, with its sign being positive in 8 of them and negative in the other 8 (References 5 and 6). If the Orbiter always departs into the lower left quadrant, and if the IUS payload weight for a particular flight were such as to require a nominal SRM-1 pitch angle of the magnitude illustrated in Figure 15, then the 8 solutions which require a negative SRM-1 pitch angle could very well be unusable. This does not mean necessarily that an acceptable flight path could not be found among the remaining 8 solutions, but the chances are certainly reduced. Given the numerous, varied, and often conflicting payload requirements and constraints that attend the selection of a nominal flight path, it does not seem to be good policy to make a choice that could in effect tie one of the flight designer's hands behind his back at the outset.

The third argument against a departure into the lower left quadrant has to do with a potential delayed-action window breakage hazard to the Orbiter. Preliminary analysis indicates that orbital mechanics can cause some of the heavier carbon particles in the SRM exhaust to reconverge on positions roughly approximated by a line parallel to the X axis in Figure 14. The nature of the phenomenon can perhaps best be described as the creation of several much-diluted "images" of the original particle source (the SRM) which pass near the origin of the LVLH coordinate system of Figure 14 recurrently at integer multiples of the Shuttle's orbit period. Each of the images is formed by the reconvergence of particles having a common geocentric orbit

*Ballasting could avoid this, but would result in a Shuttle cargo weight penalty.

period that is equal (or nearly equal) to a particular integer multiple of the Shuttle's orbit period. Rough calculations indicate that severe window (and possibly tile) breakage could result if one of these images should pass very near the Orbiter's position.

Owing to the effects of gravitational and atmospheric drag perturbations on the individual particle trajectories, a precise determination of the intensities and flight paths of the various "images" generated by a particular SRM-1 firing would be difficult. However, simple analysis indicates that exhaust particles will not reconverge at any altitude higher than that at which they were originally ejected from the SRM. Atmospheric drag will cause reconvergence to occur at progressively lower altitudes as the orbits of the individual particles decay. In light of these facts, a departure into the upper right quadrant is considered to be preferable because it would raise the Shuttle's orbit altitude and thereby tend to minimize the possibility of delayed-action window or tile breakage. At least it should eliminate the need for a complicated hazard analysis that would seem to be required if the lower left quadrant were chosen. (In this regard, it may be preferable also to choose one of the maneuver targeting solutions that requires a negative SRM-1 pitch angle. This would cause the particles in question to reconverge at lower altitudes and their orbits to decay more rapidly.)

4. TRAJECTORY AND TIMELINE DESCRIPTION

On the basis of the decisions made in the requirements analysis, a detailed trajectory was generated for the Orbiter/IUS separation phase of Flight 8. A tabulation of detailed attitude and trajectory data is contained in the Appendix.

Figure 17 shows the schedule of major events on the G.E.T. scale. Table 2 contains a tabular summary of separation phase events, correlated with both G.E.T. and with Phase Elapsed Time (P.E.T.). The latter scale, which begins at the time of IUS release from the RMS, will be the standard time reference for the remainder of the discussion in this section of the report.

Figure 18 illustrates the Orbiter's in-plane motion and approximate attitude with respect to the IUS-centered LVLH coordinate system during the interval between the initial separation maneuver at 1:00 (min:sec) P.E.T. and OMS burnout at 10:24 P.E.T. Figure 19 shows the in-plane trajectory of the Orbiter, in the same coordinate system but at a different scale, between OMS burnout and 44:24 P.E.T. The latter time corresponds approximately to SRM-1 ignition. Figure 20 is a side view of the IUS/TDRS motion relative to the Orbiter's body axes from the time of release through the end of the initial RCS burn at 1:06 P.E.T. Figure 21 is a similar view, again plotted to a different scale of the IUS/TDRS motion between the time of the RCS burn (treated here as an impulse) at 1:00 P.E.T. and OMS burnout at 10:24 P.E.T. Figure 22 is the corresponding front view of the IUS motion during that time interval. At the instant when the IUS/TDRS is released from the RMS, it was assumed that the Orbiter's +Z axis nominally would be pointed directly at the sun (see Figure 2), with all control jets inhibited and with its inertial rates nulled about all axes. It was further assumed, for the purpose of nominal trajectory calculations, that the release operation would impart no translational or rotational impulse to the IUS/TDRS. Under these idealized conditions the relative motion between the IUS/TDRS and the Orbiter is imperceptible during the one-minute interval allowed for maneuvering the RMS away from the released spacecraft and rigidizing it in preparation for the initial separation impulse.

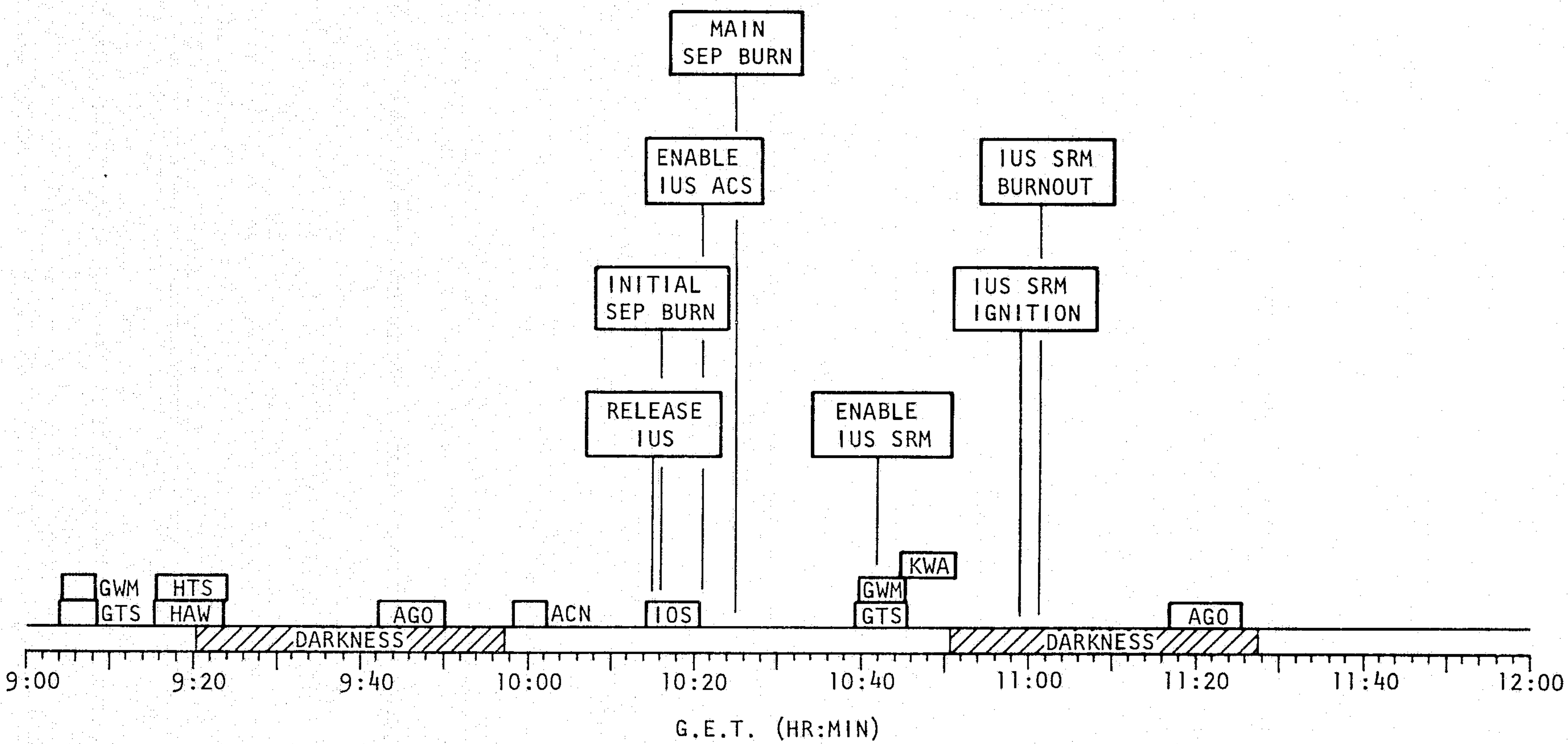

Figure 17. Separation Sequence Timeline

Table 2. Summary of Events

G.E.T. (HR:MIN:SEC)	P.E.T. (MIN:SEC)	EVENT	NOTES
10:15:00	0:00	Release IUS from RMS	Orbiter Z axis pointed at sun (Pitch -33.7, Roll 174.8, Zero inertial rate), all jets inhibited.
10:16:00	1:00	Burn -X RCS jets for 6 seconds	$\Delta q = -0.48$ deg/sec, $\Delta \dot{X}_B = -1.8$ fps, $\Delta \dot{Z}_B = 0.2$ fps
10:18:00	2:00	Begin inertial hold	VRCS, $\Delta \dot{Z}_B = -.14$ fps
10:21:00	6:00	Enable IUS attitude control	May vary ±3 minutes
10:25:00	10:00	Begin OMS burn	2 engines
10:25:24	10:24	End OMS burn	$\Delta V = 48$ fps; perhaps can reduce to 40 fps
10:40:00	25:00	Enable IUS SRM	Range $\geq$ 10 n.mi.; 27:00 - 28:00 P.E.T. probably more realistic time
10:59:00	44:00	IUS SRM ignition	Orbiter Z axis pointed toward IUS
11:01:40	46:40	IUS SRM burnout	

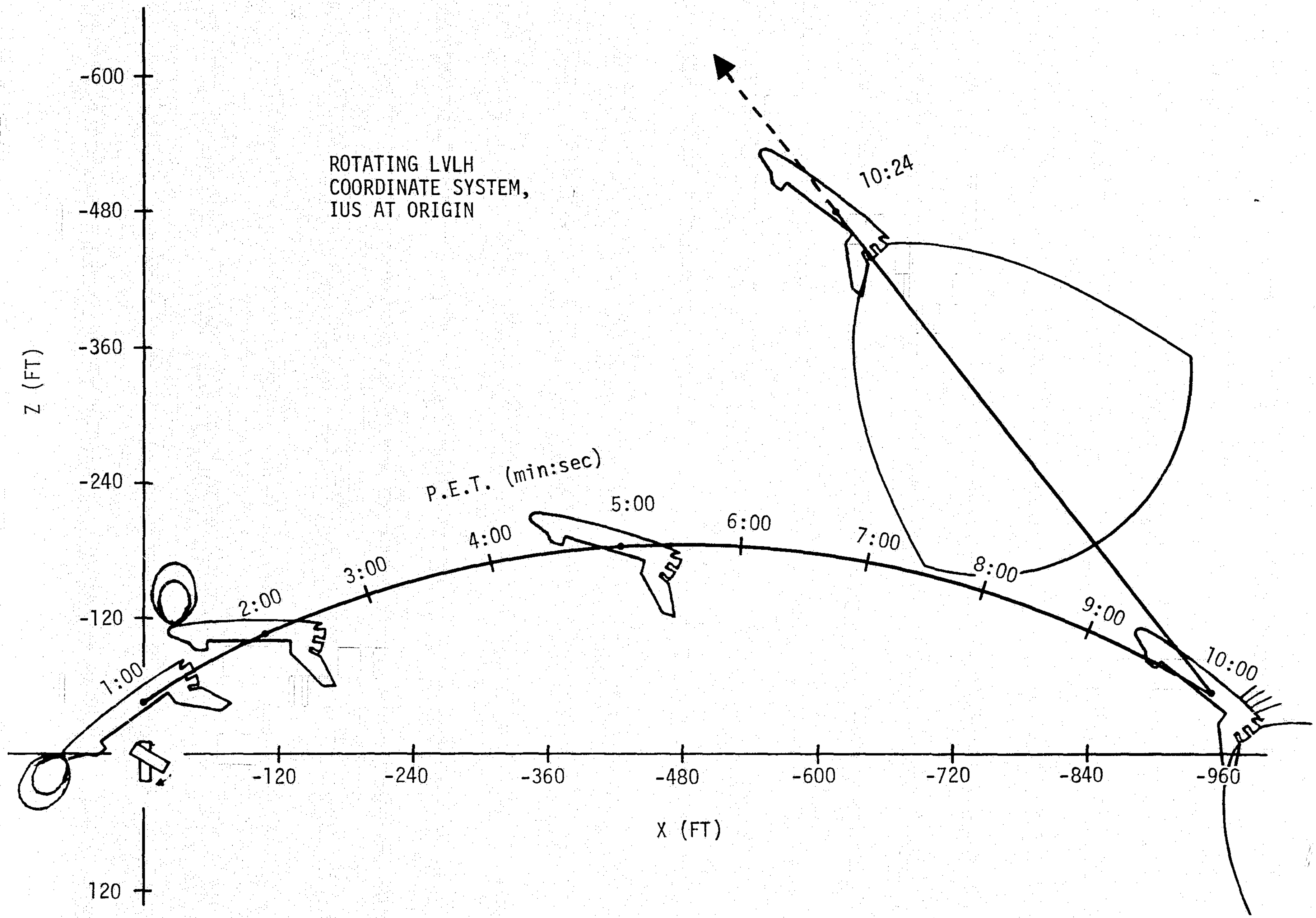

Figure 18. Orbiter Separation Trajectory (Initial Separation thru OMS Burn)

28415-H006-R0-00

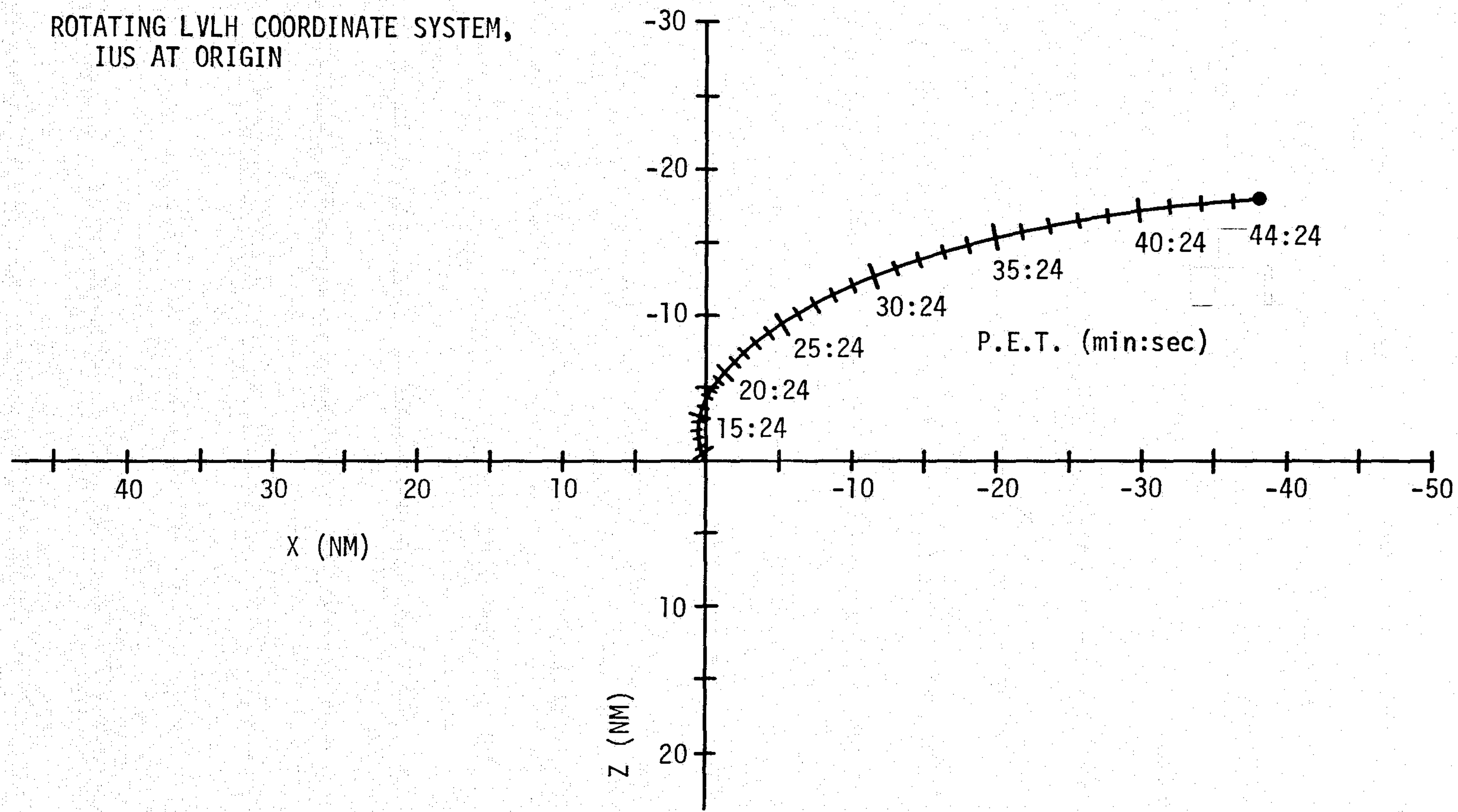

Figure 19. Orbiter Separation Trajectory (OMS Burnout to SRM-1 Ignition)

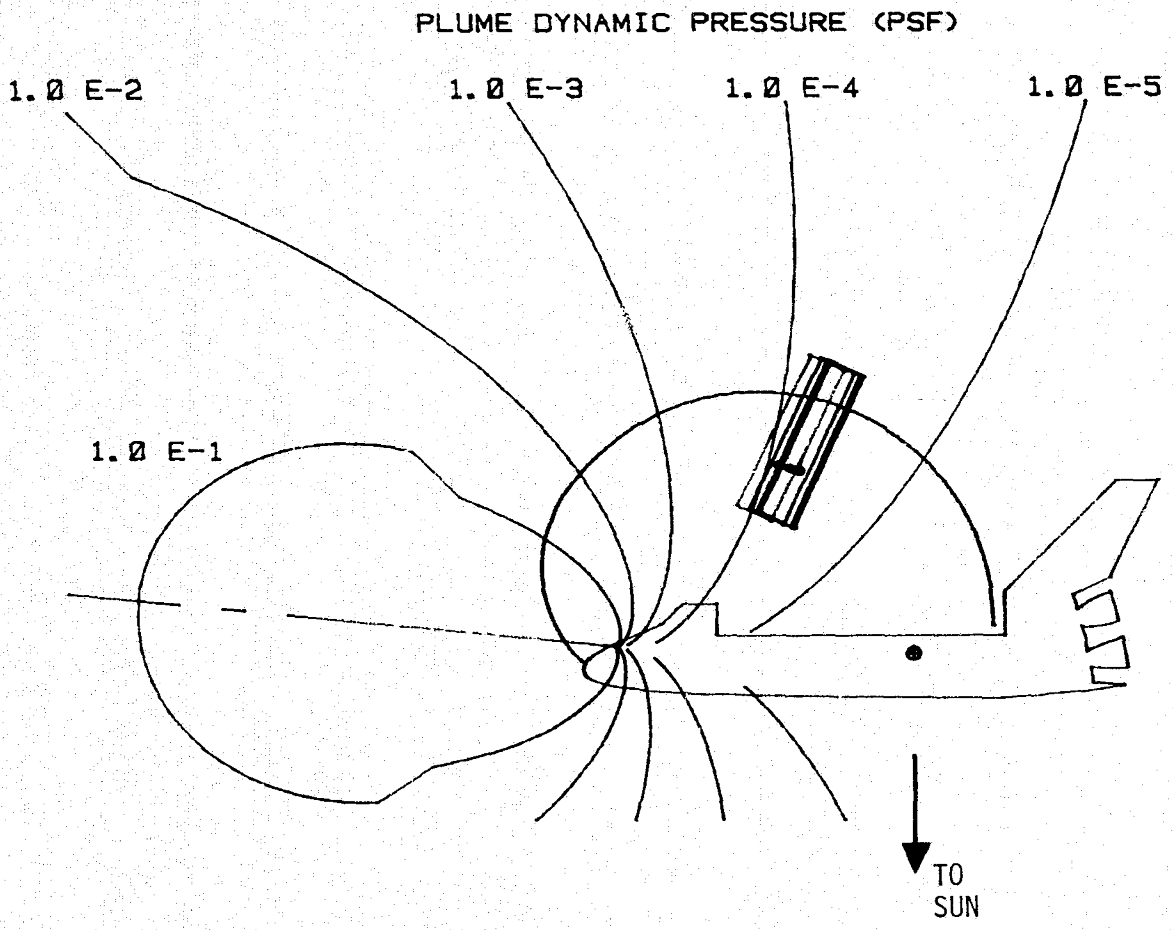

Figure 20. IUS Relative Motion (P.E.T. = 0.00 → 1:06)
and RCS Plume Contours (P.E.T. = 1:00 → 1:06)

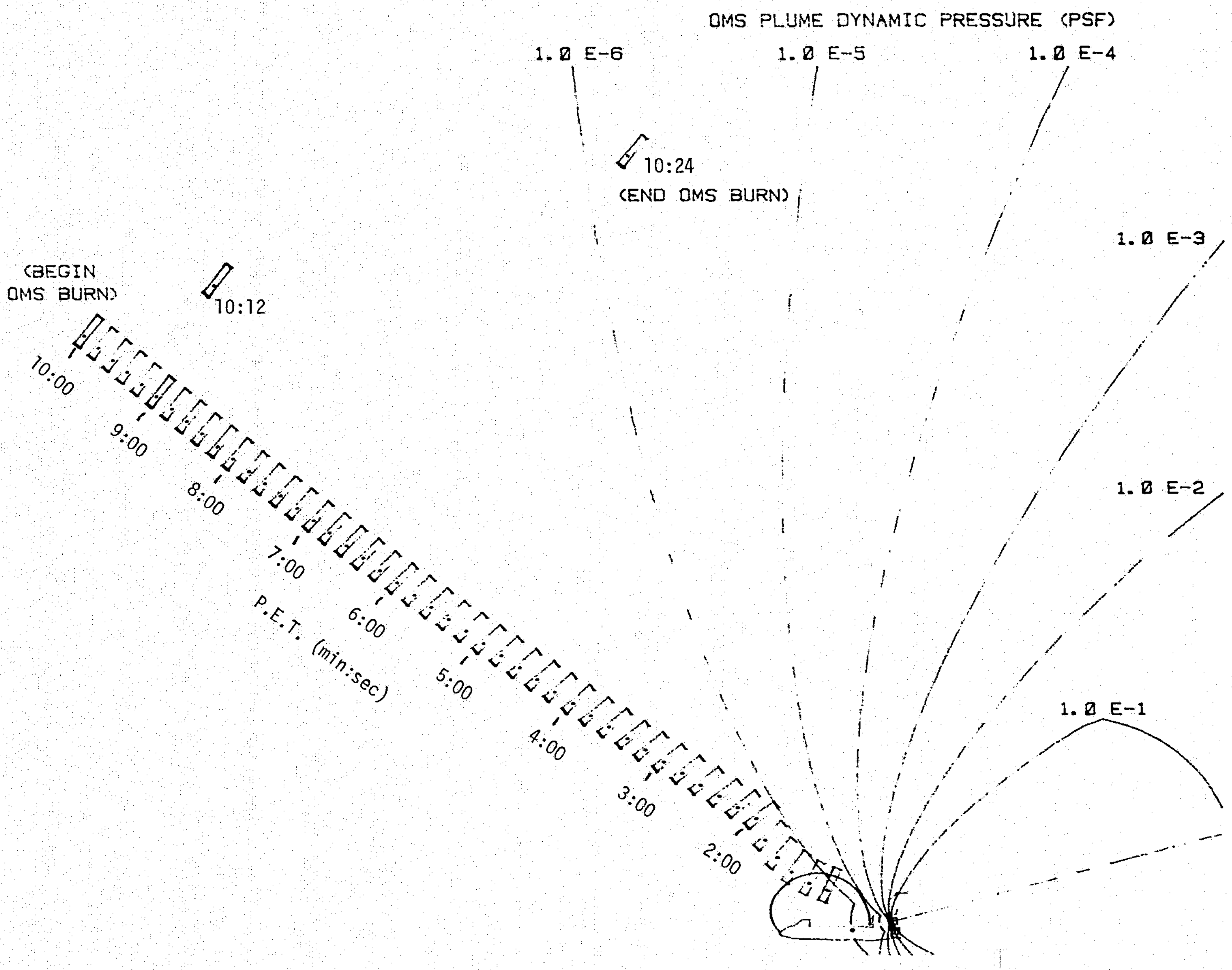

Figure 21. IUS Relative Motion (P.E.T. = 0.00 → 10:24) and OMS Plume Contours (P.E.T. = 10:00 → 10:24)

28415-H006-R0-00

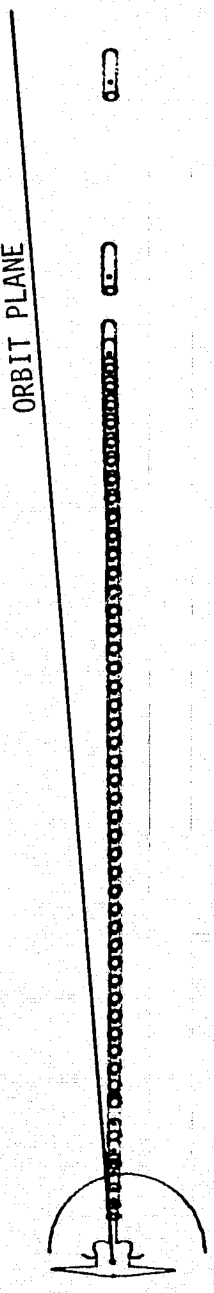

Figure 22. IUS Out-of-Plane Relative Motion (P.E.T. = 0.00 → 10:24)

The initial separation maneuver (executed at 1:00 P.E.T.) was assumed to consist of a 6-second burn of two -X RCS jets, with no cross coupling compensation. This produces an Orbiter translational velocity increment of about 1.8 feet per second, simultaneously with a negative pitch rate of approximately half a degree per second. The Orbiter attitude was allowed to drift under the influence of this rate impulse for an interval of one minute, which was calculated to produce a near-optimum inertial attitude for the execution of the subsequent OMS separation maneuver.

At 2:00 P.E.T., it was assumed that an inertial attitude hold would be initiated and maintained with the Orbiter's vernier RCS jets. A translational impulse of 0.14 feet per second, tending to nullify the initial separation impulse, was estimated to result during the cancellation of the pitch rate. If the primary RCS system were to be used at this point, inhibition of the upward-firing jets would be necessary to avoid plume impingement on the IUS/TDRS, and the undesirable translation effect (i.e., the tendency to nullify the initial separation impulse) would probably be magnified as a result of higher limit cycle rates.

During the 8-minute inertial hold (2:00 - 10:00 P.E.T.) preceding the OMS burn, the RMS is assumed to be stowed and latched down. Sometime in the interval between 3:00 and 9:00 P.E.T., an RF signal must be sent from the Orbiter to enable the IUS attitude control system. Although the appropriate antenna patterns have not been plotted, it appears in Figure 21 that there should be no problem in this regard.

If the IUS/TDRS attitude is allowed to drift for a full 9 minutes after release, gravity gradient torque will cause the nominal angle between the sun and the IUS -X axis to decrease from its initial value of 25 degrees to approximately 12 degrees (thus staying within the desired limits of 10 to 30 degrees). As indicated in Figure 20, the initial sun line angle is obtained by pitching the longitudinal axis of the IUS/TDRS configuration 25 degrees rearward with respect to the Orbiter's -Z axis prior to release. This has the effect of maximizing the depth of the payload's immersion in the shadow of the Orbiter's wing and cargo bay doors, and also tends to align its exterior surface with the radial exhaust flow streamlines from the -X RCS jets.

The latter, it is believed, should tend to minimize the disturbing torque produced by the plume.

Although the integrated effects of the RCS and OMS plumes on the IUS/TDRS have not been calculated, the dynamic pressure contours that are superimposed on the relative motion plots in Figures 20 and 21 indicate that those effects should be minimal. In both figures, it was assumed in the construction of the contours that at any given location the dynamic pressure resulting from the simultaneous firing (in the same direction) of two proximate thrusters of the same size would be twice as great as that produced by a single thruster. The plotted contours also represent plume expansion into a perfect vacuum. Since the dynamic pressure of the 1962 Standard Atmosphere in a 150-mile circular orbit is approximately 3.5×10^{-5} pounds per square foot, significant modification of the outermost dynamic pressure contours in Figures 20 and 21 can be expected as a result of thruster flowfield interaction with the atmosphere.

It can be seen in Figure 21 that the trajectory of the IUS/TDRS is such that continuous visual monitoring of its motion from the aft bulkhead closed-circuit TV camera, with its pan and tilt angles fixed, should be possible from the instant of release up to the time of OMS ignition, and through at least part of the OMS burn itself. The released spacecraft is also continuously visible through the Orbiter windshields for several minutes prior to OMS ignition. Neither of these trajectory characteristics is accidental. Visual monitoring of the released spacecraft during this critical period is considered to be essential to flight safety.

After completion of the OMS burn, it is assumed that the flight crew will point the Orbiter's -Z axis in the general direction of the IUS/TDRS, thus facilitating RF and visual contact with it, at least until the receipt of the SRM enable command by the IUS has been confirmed. Sometime prior to SRM-1 ignition, the Orbiter will have to be reoriented so that its +Z axis points in the general direction of the IUS. Several minutes are available for the execution of this rotational maneuver, which is necessary in order to prevent window breakage that would otherwise result from the impingement of carbon particles in the SRM exhaust. Figure 11 indicates that severe window breakage will occur even at the 40-mile separation distance that will exist (see Figure 19) at SRM-1 ignition time. Figure 13 shows at this distance that breakage of the high-temperature thermal tiles (which will be exposed to the plume after reorientation of the Orbiter) should be well within the limits of the damage-avoidance criterion which has been proposed in Reference 2.

Finally, it is noted that the magnitude of the OMS velocity increment might safely be reduced from 48 feet per second to something on the order of 40 feet per second. The higher value yields the 10-mile separation distance required for enabling SRM ignition at the beginning of the GTS communication opportunity. The actual transmission of the command is likely to occur at least 2 or 3 minutes later (see Figure 17). This was realized at the time that the magnitude of the velocity increment was selected. However, it is assumed that the SRM enable command would not be transmitted without confirmation from the Orbiter flight crew of successful execution of the main separation maneuver. Since the earliest opportunity for such a confirmation coincides with beginning of the GTS pass, and since some time interval is required between the burn confirmation and the transmission of the enable command, it was reasoned (erroneously, it is now believed) that the Orbiter would necessarily have to attain the required separation at or before the time of the beginning of the station pass. It is probably more reasonable to require only confirmation that the Orbiter is on a trajectory that will produce the required separation distance a few minutes later when the SRM enable command actually is to be transmitted.

5. DESIGN CRITIQUE

The development of any orbital operations technique is necessarily an iterative process involving many disciplines and organizations. The design exercise described herein represents no more than a first step in such a process. It has served its main purpose of providing insight to MPAD's flight design software requirements with respect to Orbiter/IUS proximity operations. In this regard, the key to economical and effective flight design is believed to be a capability for rapid and accurate generation of graphical displays that will facilitate not only decision-making on the part of the designer, but also lucid documentation of his rationale and of the resulting design features.

It is hoped that the data and the rationale developed in the current exercise will also be of some value in the design of the actual Orbiter/IUS separation sequences that will be executed, not only in Flight 8, but also in other Shuttle flights involving IUS deployment. With this in mind, it seems appropriate to consider the effects of certain design requirement variations.

First of all, it was learned after the completion of this exercise that the RMS probably will not be utilized in the deployment of the IUS/payload configuration. Instead, it is to be ejected by springs after being erected on its tilt table in the Orbiter's cargo bay. Since it will not be necessary to stow and latch down the RMS, it may be possible to apply the OMS velocity increment earlier than would otherwise be permissible, and thereby to reduce its magnitude. Depending on the angle of ejection and the magnitude of the spring impulse (understood to be in the range of 0.3 to 1.0 feet per second), the initial -X RCS impulse may not be required. However, whatever the magnitude and direction of the spring impulse, an OMS burn following a finite post-release coast interval will be necessary to avoid excessive plume impingement of the released spacecraft (see Section 3.1.1).

The basic features of the current design (the post-release coast interval followed by an OMS burn, departure into the upper right quadrant of Figure 14, etc.) should be applicable to the Orbiter/IUS separation phase of other flights. However, many of the detailed features will not be. Assuming the Shuttle launch azimuth and the deployment altitude do not vary, the location on the G.E.T. scale of opportunities for communication between any particular ground station and the Orbiter (or any vehicle in its proximity) will be essentially the same* for all IUS deployment flights. However, the interval between liftoff and the IUS SRM-1 burn will often be different (for example, to achieve a different TDRS placement longitude). Therefore, communication opportunities during the interval of interest here (between IUS release and execution of the SRM-1 burn) will also vary from flight to flight. As brought out in Section 3.1.1, this can have a considerable effect on the necessary magnitude of the separation velocity increment.

The position of the sun can have (as in the current example) a strong effect on the whole deployment and separation timeline, and particularly on Orbiter and IUS attitudes. Assuming it does not conflict with other flight requirements or constraints, Shuttle liftoff can always be scheduled for a time of day that will cause IUS release to occur at a fixed time relative to, say, the end of an on-orbit darkness period. Even so, the seasonal variation of the sun's declination will cause unavoidable and significant differences in sun-angle histories for flights launched at different time of the year.

These sources of variation, not to mention those related to the configuration and operating characteristics of different IUS payloads, will require the separation sequence for every flight to be individually tailored to some extent. This fact accentuates the importance of effective flight design software.

*Subject to possible differences resulting from variations in the time, magnitude, or direction of predeployment Orbiter maneuvers, such as those associated with separation from the SSUS/SBS.

REFERENCES

1. V. R. Wilmarth, "IUS/SSUS $A\ell_2O_3$ Plume Impingement Model," NASA/JSC Memorandum No. SC4-77-533, 3 November 1977 (Rev. 10 November 1977).

2. B. G. Jackson, "Minutes of Meeting: IUS and SUSS Solid Rocket Motor Exhaust Plume Analyses," NASA/JSC Memorandum No. EX32/7712-186, 30 December 1977.

3. E. C. Taylor, "Orbiter Surface Damage," MDTSCO TM No. 1.4-7-549, 27 December 1977.

4. E. C. Taylor, "Breakage Tables for Window and Tile Orbiter Surfaces due to IUS Plume Impingement," MDTSCO TM No. 1.4-7-566, 30 January 1978.

5. S. T. Chu, "A Velocity Matching Technique for IUS in Conceptual Mission Design," Enclosure 12, Third Shuttle/IUS Integration Operations Working Group Meeting Minutes, 14-16 March 1977.

6. S. T. Chu, "IUS First Burn Attitude Data," Aerospace Corp. Letter No. 77.2610.3.1-154, 15 November 1977.

APPENDIX

TRAJECTORY AND ATTITUDE DATA TABLES FOR

FLIGHT 8

IUS/ORBITER SEPARATION SEQUENCE

(ASSUMED IUS ORBIT: 150 N. MI. CIRCULAR)

ASSUMED ORBITER MASS PROPERTIES

CG LOCATION	X_o 1076.7 IN
	Y_o 0.0 IN
	Z_o 374.1 IN
WEIGHT	185 244 LB (PROBABLY TOO HEAVY)
I_{xx}	771 000 SLUG-FT^2
I_{yy}	6 013 000 SLUG-FT^2
I_{zz}	6 235 000 SLUG-FT^2
I_{yz}	0 SLUG-FT^2
I_{xz}	113 000 SLUG-FT^2
I_{xy}	-5 000 SLUG-FT^2

ASSUMED IUS/TDRSS MASS PROPERTIES

CG LOCATION	X_I 320.7 IN
	Y_I 0.0 IN (SHOULD BE -0.6)
	Z_I 0.0 IN (SHOULD BE -0.1)
WEIGHT	37 311 LB
I_{xx}	9 227 SLUG-FT^2
I_{yy}	94 014 SLUG-FT^2
I_{zz}	94 041 SLUG-FT^2
I_{yz}	0 SLUG-FT^2
I_{xz}	0 SLUG-FT^2
I_{xy}	0 SLUG-FT^2

EVENT RELEASE IUS FROM RMS

G.E.T. 10:15:00 (HR:MIN:SEC)

IUS ROTATIONAL STATE

LVLH ATTITUDE (DEG)	INERTIAL RATES (DEG/SEC)	CONTROL MODE
Pitch = -148.8	p = 0	DRIFT
Yaw = 4.7	q = 0	
Roll = -177.8	r = 0	

ORBITER ROTATIONAL STATE

LVLH ATTITUDE (DEG)	INERTIAL RATES (DEG/SEC)	CONTROL MODE
Pitch = -33.7	p = 0	DRIFT
Yaw = 0	q = 0	
Roll = 174.8	r = 0	

ORBITER TRANSLATIONAL STATE (ROTATING RELATIVE LVLH COORDINATES)

POSITION (FT)	VELOCITY (FPS)
X = 2	$\dot{X}$ = -.05
Y = -4	$\dot{Y}$ = 0
Z = -46	$\dot{Z}$ = 0

EVENT INITIAL SEP MANEUVER (IMPULSIVE -X RCS, Δq = -0.48 DEG/SEC, $\Delta \dot{X}_B$ = -1.82 FPS, $\Delta \dot{Z}_B$ = 0.20 FPS)

G.E.T. 10:16:00 (HR:MIN:SEC)

IUS ROTATIONAL STATE

LVLH ATTITUDE (DEG)	INERTIAL RATES (DEG/SEC)	CONTROL MODE
Pitch = -144.6	p = 0	DRIFT
Yaw = 4.7	q = -.006	
Roll = -177.8	r = .001	

ORBITER ROTATIONAL STATE

LVLH ATTITUDE (DEG)	INERTIAL RATES (DEG/SEC)	CONTROL MODE
Pitch = -29.9	p = 0/0*	DRIFT
Yaw = 0	q = .006/-.474*	
Roll = 174.8	r = 0/0*	

ORBITER TRANSLATIONAL STATE (ROTATING RELATIVE LVLH COORDINATES)

POSITION (FT)	VELOCITY (FPS)
X = -2	$\dot{X}$ = -.06/-1.53*
Y = -4	$\dot{Y}$ = 0/-.02*
Z = -46	$\dot{Z}$ = -.01/-1.08*

*POSTMANEUVER

EVENT   BEGIN ORBITER INERTIAL HOLD (IMPULSIVE VRCS, Δq = .472 DEG/SEC, Δr = -.001 DEG/SEC, $\Delta\dot{Z}_B$ = -.139 FPS)

G.E.T.   10:17:00 (HR:MIN:SEC)

IUS ROTATIONAL STATE

LVLH ATTITUDE (DEG)	INERTIAL RATES (DEG/SEC)	CONTROL MODE
Pitch = -140.1	p = 0	DRIFT
Yaw = 4.7	q = -.012	
Roll = -177.9	r = .001	

ORBITER ROTATIONAL STATE

LVLH ATTITUDE (DEG)	INERTIAL RATES (DEG/SEC)	CONTROL MODE
Pitch = 2.4	p = 0/0*	DRIFT/ INERTIAL HOLD*
Yaw = -2.5	q = -.472/0*	
Roll = 175.4	r = .001/0*	

ORBITER TRANSLATIONAL STATE (ROTATING RELATIVE LVLH COORDINATES)

POSITION (FT)	VELOCITY (FPS)
X = -98	$\dot{X}$ = -1.67/-1.67*
Y = -5	$\dot{Y}$ = -.02/-.01*
Z = -105	$\dot{Z}$ = -.88/-.74*

*POSTMANEUVER

EVENT BEGIN IUS INERTIAL HOLD (IMPULSIVE, Δq = .047 DEG/SEC, Δr = -.007 DEG/SEC)

G.E.T. 10:24:00 (HR:MIN:SEC)

IUS ROTATIONAL STATE

LVLH ATTITUDE (DEG)	INERTIAL RATES (DEG/SEC)	CONTROL MODE
Pitch = -98.8	p = 0/0*	DRIFT/ INERTIAL HOLD*
Yaw = 3.4	q = -.047/0*	
Roll = -178.8	r = .007/0*	

ORBITER ROTATIONAL STATE

LVLH ATTITUDE (DEG)	INERTIAL RATES (DEG/SEC)	CONTROL MODE
Pitch = 30.4	p = 0	INERTIAL HOLD
Yaw = -2.5	q = 0	
Roll = 175.4	r = 0	

ORBITER TRANSLATIONAL STATE (ROTATING RELATIVE LVLH COORDINATES)

POSITION (FT)	VELOCITY (FPS)
X = -849	$\dot{X}$ = -1.67
Y = -7	$\dot{Y}$ = 0
Z = -106	$\dot{Z}$ = 0.74

*POSTMANEUVER

EVENT BEGIN MAIN SEP BURN (2 OMS ENGINES, $\ddot{X}_B$ = 1.932 FT/SEC^2, $\ddot{Z}_B$ = 0.518 FT/SEC^2)

G.E.T. 10:25:00 (HR:MIN:SEC)

IUS ROTATIONAL STATE

LVLH ATTITUDE (DEG)	INERTIAL RATES (DEG/SEC)	CONTROL MODE
Pitch = -94.8	p = 0	INERTIAL HOLD
Yaw = 3.4	q = 0	
Roll = -178.8	r = 0	

ORBITER ROTATIONAL STATE

LVLH ATTITUDE (DEG)	INERTIAL RATES (DEG/SEC)	CONTROL MODE
Pitch = 34.4	p = 0	INERTIAL HOLD
Yaw = -2.5	q = 0	
Roll = 175.4	r = 0	

ORBITER TRANSLATIONAL STATE (ROTATING RELATIVE LVLH COORDINATES)

POSITION (FT)	VELOCITY (FPS)
X = -945	$\dot{X}$ = -1.55
Y = -7	$\dot{Y}$ = 0
Z = -55	$\dot{Z}$ = 0.94

EVENT END MAIN SEP BURN

G.E.T. 10:25:24 (HR:MIN:SEC)

IUS ROTATIONAL STATE

LVLH ATTITUDE (DEG)	INERTIAL RATES (DEG/SEC)	CONTROL MODE
Pitch = -93.2	p = 0	INERTIAL HOLD
Yaw = 3.4	q = 0	
Roll = -178.8	r = 0	

ORBITER ROTATIONAL STATE

LVLH ATTITUDE (DEG)	INERTIAL RATES (DEG/SEC)	CONTROL MODE
Pitch = 36.0	p = 0	INERTIAL HOLD
Yaw = -2.5	q = 0	
Roll = 175.4	r = 0	

ORBITER TRANSLATIONAL STATE (ROTATING RELATIVE LVLH COORDINATES)

POSITION (FT)	VELOCITY (FPS)
X = -620	$\dot{X}$ = 28.16
Y = -43	$\dot{Y}$ = -3.03
Z = -478	$\dot{Z}$ = -36.61